https://doi.org/10.5194/egusphere-2026-5347
Preprint. Discussion started: 9 September 2026

EarthCARE Commissioning Calibration and Validation Campaign in Ottawa (ECALOT): An Integrated Approach to Multi-level EarthCARE Validation

Zhipeng Qu[1], Cuong Nguyen[2], Paloma Borque[2], Alexei Korolev[1], Howard W. Barker[1], Keyvan Ranjbar[2], Lei Liu[3], Zen Mariani[1], Meriem Kacimi[1], Melissa Cholette[1], Ivan Heckman[1], Kenny Bala[2], Natalia Bliankinshtein[2], Leonid Nichman[2], Benjamin Riot-Bretêcher[3], Yi Huang[3], Jason N. S. Cole[1], Raphaël Peroni[4], Stephen Holden[1], Robert Reed[1], Robert Crawford[1], Daniel Michelson[1], Eve Bigras[3], Michael Wheeler[1], John Gyakum[3], Jason A. Milbrandt[1], Julie M. Thériault[4], Kaley A. Walker[5], Mengistu Wolde[2], Jean-Pierre Blanchet[4], Yann Blanchard[4], Jonas von Bismark[6], Rob Koopman[6], Montserrat Piñol Solé[6], Bernat Puigdomènech Treserras[3], Robin J. Hogan[7], and Shannon L. Mason[7]

[1]Environmental Research and Modelling Directorate, Environment and Climate Change Canada, Toronto, ON, Canada
[2]Flight Research Laboratory, National Research Council Canada, Ottawa, ON, Canada
[3]Department of Atmospheric and Oceanic Sciences, McGill University, Montreal, QC, Canada
[4]Department of Earth and Atmospheric Sciences, Université du Québec à Montréal, Montreal, QC, Canada
[5]Department of Physics, University of Toronto, Toronto, ON, Canada
[6]European Space Agency, Noordwijk, Netherlands
[7]European Centre for Medium-Range Weather Forecasts, Reading, UK

Correspondence to: Zhipeng Qu (zhipeng.qu@ec.gc.ca)

Abstract. The EarthCARE Commissioning Calibration and Validation Campaign in Ottawa (ECALOT) was a dedicated airborne and surface-based campaign designed to support the calibration and validation of Level 1 and Level 2 products from the EarthCARE satellite mission. The campaign was conducted between October 2024 and March 2025 in eastern Canada, primarily in the regions surrounding Ottawa and Montreal. Airborne observations were carried out using the National Research Council Canada (NRC) Convair-580 research aircraft, equipped with remote sensing instruments analogous to those flown on EarthCARE, including a nadir/zenith/side-looking 94 GHz cloud radar system with Doppler capability and zenith/nadir-pointing 355 nm elastic lidars, together with a comprehensive suite of in situ cloud and aerosol probes. Complementary surface-based observations were obtained at a primary site at the Ottawa Macdonald-Cartier International Airport and two additional climate sentinel stations in the Montreal region, providing continuous ground-based reference measurements of surface radiation, atmospheric thermodynamic profiles, precipitation, and other meteorological variables.

A total of seven research flights were conducted, sampling a range of mid-latitude continental cloud conditions, including stratocumulus, multilayer cloud systems, and nimbostratus associated with liquid- or solid-phase precipitation. The ECALOT sampling strategy was designed to integrate airborne and surface-based in situ and remote-sensing observations collected along and offset from EarthCARE's ground track, while accounting for temporal offsets relative to the satellite overpass. Together,

https://doi.org/10.5194/egusphere-2026-5347
Preprint. Discussion started: 9 September 2026

the ECALOT campaign provides coordinated multi-platform observations that enable evaluation of active sensor measurements, radar-lidar-imager synergy, representation of liquid, ice and mixed-phase clouds, three-dimensional scene construction, and radiative closure across EarthCARE's data processing chain, while also providing observational constraints for improving the representation of mixed-phase clouds and their radiative effects in numerical models.

1. Introduction

Clouds and aerosols are key atmospheric constituents that regulate the Earth's energy budget and participate in complex microphysical, dynamical, and chemical processes that regulate precipitation, atmospheric composition, and climate variability. A quantitative understanding of the physical processes governing clouds and aerosols, as well as their interactions with radiation, is essential for improving weather forecasting and reducing uncertainties in climate projections. The central role of cloud-aerosol-radiation interactions has been explicitly highlighted in the Decadal Strategy for Earth Observation from Space (NASEM, 2018). Previous satellite missions, notably CloudSat (Stephens et al., 2002) and Cloud-Aerosol Lidar and Infrared Pathfinder Satellite Observations (CALIPSO) (Winker et al., 2010), which were part of the A-Train satellite constellation, demonstrated both the scientific value of long-term vertically resolved observations of clouds and aerosols and the technical feasibility of active remote sensing from space. However, these missions ceased operations in 2023, leaving a critical observational gap.

The EarthCARE satellite, a joint mission of the European Space Agency (ESA) and the Japan Aerospace Exploration Agency (JAXA), was launched on 28 May 2024 (Illingworth et al., 2015; Wehr et al., 2023; Eisinger et al., 2024). The mission aims to advance quantitative understanding of interactions among clouds, aerosols, and radiation and their role in the Earth's climate system. By combining active and passive remote sensing from space, it delivers vertically resolved observations of cloud and aerosols together with coincident radiative measurements. This synergistic observing capability enhances the characterization of cloud/aerosol structure, geophysical properties, and provides a foundation for integrated studies of cloud-aerosol-radiation interactions (Illingworth et al., 2015; Seiki et al., 2025; Xu et al., 2025; Galfione et al., 2025; Khaykin et al., 2026; Aoki et al., 2026, Mayer et al., 2026), while supporting efforts to improve their representation in numerical weather prediction (NWP) and Earth system models (Fielding and Janiskova, 2023; Roh et al., 2024; Feenstra et al., 2025, Cholette et al. 2026).

Mid-latitude cloud systems involve a range of physical processes that remain poorly understood or inadequately represented in numerical models, such as mixed-phase processes within predominantly ice clouds (Korolev and Milbrandt, 2022; Cholette et al. 2026), high ice water content conditions and secondary ice production (Korolev and Leisner, 2020; Rugg et al, 2022; Huang et al., 2021, 2022; Qu et al., 2022, 2025; Lachapelle et al., 2024), organization of marine stratocumulus (Xu et al., 2025; Mayer et al., 2026), the three-dimensional (3D) structure of cloud fields (Barker et al. 2011, 2012, 2014; Qu et al., 2023) and the associated 3D radiative effects (Barker et al., 2003; Várnai & Marshak, 2003; Hogan et al., 2019; Veerman et al., 2022, Villefranque et al., 2021). Through its combined active and passive instruments, EarthCARE provides integrated observations

https://doi.org/10.5194/egusphere-2026-5347
Preprint. Discussion started: 9 September 2026

with considerable potential to advance our understanding of these processes. Realizing this scientific potential, however, depends on the accuracy and consistency of a suite of products, including single-instrument measurements and retrievals, composite and multi-instrument synergistic retrievals of cloud and aerosol properties, scene-construction products, and radiation products.

Calibration and validation (cal/val) activities are therefore essential to the EarthCARE mission. In accordance with the principles outlined in the Best Practice Protocol for the Validation of Aerosol, Cloud, and Precipitation Profiles (ACPPV; Amiridis et al., 2025), independent observations are required not only to validate Level 1 calibrated measurements and Level 2 processed instrument products, but also to assess geophysical retrieval accuracy, evaluate assumptions underlying the retrieval algorithms, quantify uncertainties, and examine radiative consistency across the product chain and throughout different regions.

Coordinated airborne and surface-based campaigns play a critical role in EarthCARE's cal/val. Airborne platforms provide high-resolution remote-sensing and in situ measurements that serve as independent reference observations for evaluating instrument performance and geophysical retrievals of cloud and aerosols along satellite ground tracks. Surface-based observations provide continuous temporal coverage, supporting characterization of scene evolution and background atmospheric conditions, while also providing comparison datasets in the lower atmosphere, where satellite retrievals can be challenged by signal attenuation, surface contamination, and limited sensitivity. Together, these coordinated observations and associated analyses address best-practice validation recommendations and improve the quality and robustness of EarthCARE's measurements and geophysical retrievals (ESA, 2024; Amiridis et al., 2025).

Following launch, EarthCARE has been supported by extensive international cal/val efforts involving coordinated airborne and ground-based observations across diverse atmospheric regimes (Kubota et al., 2026). Examples of airborne campaigns supporting EarthCARE cal/val include PERCUSION and CELLO in the tropical Atlantic (Groß et al., 2026; Stevens et al., 2026); MORECALVAL (François et al., 2025) and VERIFY (Mroz et al., 2025) in mid-latitude environments; ARCSIX, COMPEX-EC (van Gelder et al., 2025) and PONEX (Walker et al., 2025, Mariani et al., 2026) at high latitudes; and NightBLUE (Hemminga et al., 2025) and NAWDIC-DICHOTOMI (François et al., 2026) over the North Atlantic; HALO-South over the Southern Ocean (Menekay et al., 2026); and PACE-PAX over the eastern Pacific and western North America (Cetinić et al., 2024). These airborne activities have been complemented by ground-based validation efforts, including the PollyNET/ACTRIS lidar network for validation of ATLID aerosol and cloud profiling products (Baars et al., 2026) and the RACE-ECV campaign which focuses on EarthCARE radiative closure using high-accuracy surface radiation, aerosol, and cloud observations (Kazadzis et al., 2026). Full campaign/network names are provided in Appendix A.

In this context, the EarthCARE Commissioning Calibration and Validation Campaign in Ottawa (ECALOT) was conducted from October 2024 to March 2025 in the Ottawa-Montreal region of eastern Canada, spanning the second half of the commissioning phase and the early operational phase of the EarthCARE mission. Led by Environment and Climate Change

https://doi.org/10.5194/egusphere-2026-5347
Preprint. Discussion started: 9 September 2026

Canada (ECCC) in partnership with the National Research Council Canada (NRC), McGill University, Université du Québec à Montréal (UQAM), the University of Toronto, and ESA, the six-month campaign combined ground-based observations with flexible, targeted aircraft operations to support EarthCARE cal/val. Research flights were conducted selectively around suitable EarthCARE overpasses and meteorological conditions, with particular emphasis on mid-latitude continental cloud and aerosol regimes.

Airborne remote sensing and in situ measurements were coordinated with EarthCARE overpasses to enable direct comparison along underflight tracks, while also providing off-nadir sampling to support validation of 3D scene construction and aircraft-level radiative closure assessments. Fixed ground-based observations provided background characterization, independent boundary radiative constraints, and additional support for scene construction validation. Together, these complementary multi-platform observations deliver independent measurements across multiple seasons and atmospheric regimes, enabling evaluation of Level 1 calibrated measurements, Level 2 processed measurements and geophysical retrievals under a range of meteorological and surface conditions.

In addition to its cal/val role, the coordinated observations provide a valuable opportunity to investigate cloud microphysical processes that remain challenging to represent in numerical models, particularly those governing the formation, evolution, and persistence of supercooled liquid layers embedded within ice-dominated clouds. The combination of EarthCARE radar-lidar observations with airborne remote-sensing measurements and in situ microphysical observations enables detailed characterization of the structure of these layers. These complementary observations provide important constraints on the underlying microphysical processes, thereby supporting improved representation of mixed-phase clouds in NWP and climate models.

ECALOT also supports multi-level radiative closure studies by combining radiative measurements from the surface, aircraft level, and from space. Surface-based observations provide bottom-of-atmosphere constraints, while airborne measurements offer estimates of radiative quantities within the cloud layer. When combined with EarthCARE's top-of-atmosphere (TOA) radiative observations and retrieved cloud and aerosols profiles, these measurements enable a more complete assessment of radiative consistency across the atmospheric column. This integrated framework allows evaluation of how well retrieved cloud and aerosol properties reproduce observed radiative quantities and helps identify discrepancies associated with the vertical cloud-phase structure, retrieval methods, microphysical assumptions, and three-dimensional scene construction.

This paper is structured as follows. Section 2 provides an overview of the ECALOT campaign. Section 3 describes the EarthCARE validation requirements and the corresponding campaign design. Section 4 details the instrumentation and observational strategy, and Section 5 summarizes the dataset and quality control procedures. Section 6 discusses the relevance of ECALOT to EarthCARE cal/val and science applications, followed by conclusions in Section 7.

https://doi.org/10.5194/egusphere-2026-5347
Preprint. Discussion started: 9 September 2026

2. Overview of ECALOT campaign

The ECALOT campaign combined coordinated airborne and surface-based observations to provide a comprehensive observational framework relevant to EarthCARE products, enabling cal/val of several Level 1 and Level 2 products. Airborne observations were conducted using the NRC Convair-580 research aircraft, which has been used extensively for atmospheric research over the past several decades (e.g., Lawson et al., 1993; Cober et al., 2001; Barker et al., 2008; McFarquhar et al., 2011; Qu et al., 2018; Liggio et al., 2019; Wolde et al., 2019; Nguyen et al., 2022; Minder et al., 2023; Kollias et al., 2025). The aircraft was equipped with W-, X- and Ka- band cloud radars, 355 nm elastic lidars, in situ cloud and aerosol probes, atmospheric state sensors, and an airborne far-infrared radiometer. These measurements provided active and passive remote sensing observations together with in situ microphysical and thermodynamic data.

Surface-based observations were conducted at fixed sites within the same region and provided continuous or near-continuous measurements of radiative properties, thermodynamic profiles, precipitation occurrence and classification, cloud base height, and aerosol layer detection, offering sustained temporal context for the interpretation of airborne observations and coincident EarthCARE observations.

2.1 Campaign objectives

The primary objective of ECALOT is to support EarthCARE cal/val activities through coordinated airborne and ground-based observations and associated analyses. Specific objectives of the campaign include:

- cal/val of EarthCARE Level 1 and Level 2 radar and lidar products through direct comparison with airborne and ground-based remote sensing observations;
- assessment of EarthCARE Level 2 geophysical retrievals, with emphasis on vertically resolved cloud properties, structure, and phase, as well as aerosol layer detection, supported by in situ and remote sensing observations and radiative closure analyses;
- evaluation of EarthCARE scene construction algorithms through coordinated airborne and ground-based observations;
- investigation of the benefit of multi-level radiative closure (surface, airborne, and top-of-atmosphere) in improving retrieval consistency and diagnosing sources of radiative discrepancies;
- provision of observational constraints to support the development and improvement of advanced cloud microphysical parameterizations in NWP models;
- Identify current cal/val gaps and potential goals for future campaigns.

https://doi.org/10.5194/egusphere-2026-5347
Preprint. Discussion started: 9 September 2026

2.2 Campaign region and temporal coverage

ECALOT was conducted in the Ottawa-Montreal region of eastern Canada, a mid-latitude continental environment characterized by pronounced seasonal variability. The region experiences a wide range of atmospheric conditions, including seasonal transitions between convective and stratiform cloud systems, frequent mixed-phase clouds, and aerosol variability influenced by both local emissions and long-range transport (Isaac et al., 2005; O'Neill et al., 2006; Barker et al., 2008; Kovacs et al., 2016; Sioris et al., 2017; Cholette et al., 2020; Wijayarathne et al., 2020; Minder et al., 2023; Boudala et al., 2025). These characteristics make the region particularly well suited for evaluating retrieval performance across diverse cloud and aerosol conditions.

Surface conditions also vary substantially throughout the year, including transitions between snow-covered and snow-free periods. The region encompasses heterogeneous landscapes and topographic settings, including river valleys, mountainous terrain, dense urban areas, and agricultural land. This diversity is particularly relevant to the evaluation of radiative measurements.

Airborne and surface-based observations were conducted between October 1, 2024 and March 25, 2025. During this period, seven research flights were carried out, while surface sites operated continuously or near-continuously, providing coverage across nearly three seasons. This temporal extent enabled sampling of diverse mid-latitude continental cloud regimes, including cumulus and stratocumulus clouds during warmer and transitional periods, as well as nimbostratus associated with liquid- or solid-phase precipitation. The campaign therefore captured clouds spanning liquid, ice, and mixed-phase conditions and exhibiting diverse microphysical characteristics. The extended temporal coverage provides a consistent observational reference for evaluating EarthCARE products under a broad range of atmospheric conditions.

2.3 Scope of EarthCARE products addressed

EarthCARE's scientific objective is realized through a system that integrates a 355 nm atmospheric lidar (ATLID), a W-band Doppler cloud radar (CPR), a multispectral imager (MSI), and a broadband radiometer (BBR) to produce collocated profiles of aerosols, clouds, and precipitation together with TOA radiances and fluxes (Wehr et al., 2023). Achieving this objective requires validation at multiple stages of the processing chain. At Level 1, this includes calibration and validation of each instrument's fundamental measurements (Wehr et al., 2023; Eisinger et al., 2024). At Level 2, it includes both processed instrument measurements (Kollias et al., 2023; Donovan et al., 2024) and geophysical retrievals, including single-instrument and their composite products (Cole et al., 2023; Mroz et al., 2023; Wandinger et al., 2023; Docter et al., 2024; Donovan et al., 2024, Hünerbein et al., 2024), as well as multi-instrument synergy products (Irbah et al., 2023; Haarig et al., 2023; Mason et al., 2023). The latter depends on physically consistent CPR-ATLID-MSI scene interpretation.

A further requirement is radiative self-consistency or radiative closure. Radiative transfer simulations (Cole et al., 2023), driven by retrieved and constructed 3D atmospheric scenes (Qu et al., 2023), are evaluated against independent broadband radiance

https://doi.org/10.5194/egusphere-2026-5347
Preprint. Discussion started: 9 September 2026

and flux measurements from BBR (Velázquez Blázquez et al., 2024). Radiative closure is therefore defined as a performance requirement within the mission verification framework (Barker et al., 2025).

The ECALOT campaign is designed to address EarthCARE products across successive stages of the processing chain. At Level 1, ECALOT supports the evaluation of calibrated CPR reflectivity and Doppler velocity measurements, ATLID backscatter and depolarization ratio measurements, and associated auxiliary temperature and humidity fields used as inputs to downstream products. At Level 2, the campaign provides constraints for both radar and lidar measurement products and geophysical retrievals of cloud and aerosol properties, including single-instrument composite products and multi-instrument synergy products. In addition, coordinated airborne and surface-based radiative observations enable independent radiative closure assessments with different viewing geometries. By spanning measurements from calibrated observations to retrieved geophysical and radiative quantities, ECALOT supports calibration and validation across multiple stages of the EarthCARE processing chain.

3. ECALOT campaign design

3.1 EarthCARE measurement and validation requirements

Cal/val activities must address both individual products at different levels and the internal consistency across EarthCARE's processing chain. At Level 1, validation requirements address the performance of calibrated satellite measurements and the accuracy of auxiliary atmospheric variables. In accordance with ACPPV best-practice principles (Amiridis et al., 2025), validation relies on independent reference observations and must account for differences in viewing geometry, spatial resolution, and sampling characteristics between spaceborne and correlative measurements. Appropriate collocation strategies and representativeness considerations are therefore essential.

At Level 2, validation requirements address both processed measurement-based products and retrieved geophysical variables. This includes evaluation of cloud and aerosol detection, cloud microphysical properties, vertical and horizontal structure, aerosol detection and type, and other derived quantities. Validation also includes comparison with independent observations and assessment of consistency between single-sensor composite and multi-sensor synergistic products across a range of atmospheric conditions.

Radiative products impose additional requirements on the coherent representation of cloud and aerosol properties, atmospheric state, and surface conditions. The accuracy of simulated radiative quantities depends on the combined performance of measurement calibration, retrieval algorithms, scene construction, surface properties, auxiliary atmospheric inputs, and the radiative transfer method itself. Because of this, radiative closure assessment represents an end-to-end evaluation of the processing chain. In addition to the operational radiative closure assessment conducted using BBR measurements, independent

https://doi.org/10.5194/egusphere-2026-5347
Preprint. Discussion started: 9 September 2026

closure assessments using radiative observations from surface and airborne platforms provide additional constraints on EarthCARE's system-level consistency.

In addition to product-level requirements, EarthCARE cal/val must address performance across a broad range of cloud and aerosol scene types. Instrument performances vary substantially between liquid, ice, and mixed-phase clouds and depend strongly on cloud vertical and horizontal structure (Irbah et al., 2023; Mason et al., 2024). Similarly, aerosol detectability and typing are strongly influenced by atmospheric conditions (Irbah et al., 2023; Wandinger et al., 2023). Validation activities must therefore encompass diverse cloud-aerosol regimes to ensure that product quality and consistency are evaluated beyond a limited set of atmospheric conditions.

Satellite-aircraft-surface comparisons are inherently subject to differences in sampling geometry and temporal representativeness. EarthCARE observes atmospheric scenes at high air speed, whereas airborne observations are acquired at substantially lower speeds, and surface-based measurements are typically offset from the exact satellite ground track. As a result, direct point-to-point comparisons are not always feasible, and validation activities must account for acceptable tolerances in space and time. Robust evaluation therefore requires sampling and comparison strategies that consider atmospheric variability, spatial averaging, and temporal matching, as well as statistical approaches, rather than relying solely on exact collocation.

Taken together, these requirements indicate that comprehensive EarthCARE cal/val ideally span multiple stages of the processing chain, from low-level instrument measurements to higher-level synergistic and radiative closure products. Such evaluation requires coordinated observations that provide vertically resolved measurements, detailed characterization of cloud and aerosol structure across diverse scene types, radiative measurements at relevant levels (surface or aircraft), and sufficient atmospheric context, while accounting for spatial and temporal sampling differences between satellite, airborne, and surface-based observations.

3.2. Design Principles of the ECALOT Campaign

The ECALOT campaign employed coordinated airborne and surface-based observations that collectively support EarthCARE's evaluation across multiple product levels. Rather than focusing on individual instruments or specific retrievals, ECALOT adopts an end-to-end perspective, enabling assessment from Level 1 remote sensing measurements and auxiliary atmospheric data through Level 2 processed measurements, cloud and aerosol retrievals, 3D scene construction, and radiative products.

ECALOT utilized combined active and passive remote sensing measurements together with in situ observations to provide complementary information on cloud and aerosol properties, as well as radiative quantities. Airborne active remote sensing measurements provide vertically resolved observations that are directly comparable to EarthCARE's Level 1 CPR and ATLID products, while high-quality in situ measurements collected within individual cloud and aerosol layers serve as independent

https://doi.org/10.5194/egusphere-2026-5347
Preprint. Discussion started: 9 September 2026

reference data for the evaluation of EarthCARE's Level 2 geophysical retrievals. Coordinated airborne and surface-based radiative measurements directly constrain EarthCARE's Level-2 radiative products and, through radiative closure analyses, provide additional constraints on cloud and aerosol retrievals. This integrated observational approach supports the cal/val of a broad range of EarthCARE products across both EarthCARE Level 1 and Level 2 data processing chain.

ECALOT further incorporates targeted sampling strategies to support validation of EarthCARE's scene construction products. Dedicated flight patterns and varying radar pointing geometries are employed to enhance observations of cloud and aerosol structures in off-nadir regions. Comparisons between airborne observations and EarthCARE-constructed cloud properties in these off-nadir regions enable quantitative evaluation of the performance of the scene construction algorithm.

Sampling a broad range of cloud scene types is another key design principle of ECALOT. Observations spanning multiple seasons allow sampling of liquid, ice, and mixed-phase clouds under varying thermodynamic environments, which is essential for robust evaluation of both single-sensor, composite and synergistic EarthCARE retrievals.

Finally, the ECALOT design explicitly accounts for spatial and temporal mismatches between satellite, airborne, and surface-based observations by emphasizing sampling strategies that minimize temporal offsets and geometric mismatches between platforms. Underflight legs are designed with limited duration to minimize scene evolution during the satellite overpass, and off-nadir sampling is conducted within short temporal windows while accounting for wind direction to better align sampled air masses. When feasible, large-scale stratiform cloud systems provide an additional advantage by offering greater horizontal continuity, further reducing sensitivity to small spatial offsets and temporal sampling differences.

4. Instrumentation and observational strategy

4.1. Airborne instrumentation

Table 1 provides a full list of all instruments integrated into the NRC Convair-580 during ECALOT, including active remote sensing systems, passive radiometers, in situ cloud and aerosol probes, and atmospheric state instruments. Instruments operated during selected flights are identified in the Notes column.

Table 1: List of sensors integrated into the NRC aircraft for the ECALOT campaign. For some instruments, the manufacturer name is noted (such as SkyTech, Goodrich, DMT, SPEC, LR-Tech)

Instrument	Measurement Principle	Measured Parameters	Measurement Details & Notes
Remote Sensing Instruments			
NRC Airborne W-band (NAW) radar	Active cloud radar (94.05 GHz)	Radar reflectivity factor and Doppler velocity	Fuselage, nadir/zenith/side-pointing
NRC Airborne X-band (NAX) radar	Active cloud radar (9.41 GHz)	Radar reflectivity factor and Doppler velocity	Fuselage, nadir/zenith-pointing

https://doi.org/10.5194/egusphere-2026-5347
Preprint. Discussion started: 9 September 2026

ProSensing Ka-Band Radar (KPR)	Active cloud radar (35 GHz)	Radar reflectivity factor and Doppler velocity	Wingtip, nadir/zenith-pointing, available for Flight 4 & 5
355 nm Airborne Elastic Cloud Lidar (AECL)	Elastic backscatter lidar	Co- and cross-polar lidar backscattering powers	Cabin, nadir/zenith-pointing, nadir-pointing only available for Flight 1-5
Far-Infrared Radiometer-2 (FIRR-2)	Passive far-infrared radiometer	Radiances spectrally integrated over 8 spectral bands from 7.9 µm to 27.5 µm, together with the corresponding brightness temperatures derived for each band; the 15–27.5 µm range corresponds to the far-infrared region.	Cabin, nadir-viewing, available for Flight 6-7. Instrument built by LR-Tech.
High Spectral Resolution Airborne Microwave Sounder (HiSRAMS)	Passive hyperspectral radiometers	Temperature and humidity	Wingtip, available for Flight 1-3, 6-7
Cloud In Situ Instruments			
SkyTech Nevzorov (Analog)	Hot-Wire	Liquid water content (LWC) and total water content (TWC), 0.01-3 g m^{-3}	
Goodrich Icing Detector	Vibrating icing rod	Icing presence/icing indicator Threshold≈0.01 g m^{-3}, T<-4°C	
DMT Cloud Droplet Probe (CDP-2)	Forward scattering probe	Cloud droplet size distribution (~2–50 µm)	
SPEC 2D-S (Stereo) Probe	Optical array imaging probe	Particle size distribution (10–1280 µm); ~10 µm nominal pixel resolution	
SPEC High Volume Precipitation Spectrometer-3 (HVPS-3)	Optical array imaging probe	Particle size distribution (150–19,200 µm); 150 µm nominal pixel resolution	Available for Flight 1-5
SPEC High Volume Precipitation Spectrometer-4 (HVPS-4)	Optical array imaging probe	Particle size distribution (150–19,200 µm); 150 µm nominal pixel resolution	Available for Flight 6-7
SPEC Cloud Particle Imager (CPI)	High-resolution grayscale imaging probe	High-resolution particle images (~15–2000 µm); 2.3 µm nominal pixel resolution	
Aerosol In Situ Instruments			
Cloud Condensation Nuclei counter-100 (CCNc-100)	Cloud condensation nuclei counter	CCN concentration at prescribed supersaturations	
Ultra-High Sensitivity Aerosol Spectrometer (UHSAS)	Light scattering	Aerosol particle size distribution (~60–1000 nm)	
Atmospheric State Instruments			

https://doi.org/10.5194/egusphere-2026-5347
Preprint. Discussion started: 9 September 2026

RMNT Pressure Transducer	Differential and static pressure sensing	Static and dynamic pressure	
RMNT TAT	Total air temperature (TAT) probe	Temperature	
RMNT 858 Air Data Probe (ADP)	Aircraft data probe (multi-hole pressure probe)	Pressures, incidence angles	Independent 3D winds when combined data with cabin mounted Inertial Measurement Unit (IMU)
Licor 848a or Licor 7000	Non-dispersive infrared (NDIR) gas analyser	H2O concentrations, CO_2, Dew Point	Cabin
Global Positioning System (GPS)	Satellite-based positioning system	Aircraft position (latitude, longitude), altitude, ground speed, time	Combined with IMU via Kalman filtering; real-time and post-processed solutions available

4.2. Surface-based instrumentation

Surface observations provide a comprehensive suite of coordinated active and passive remote sensing measurements and in situ observations within the satellite swath. Three surface sites supported the ECALOT campaign: Ottawa Macdonald-Cartier International Airport (YOW; 45°19′38.1″N, 75°39′49.4″W, 112.84 m ASL); the Montreal site, consisting of two locations: the rooftop of Burnside Hall at McGill University (45°30'16.88"N, 73°34'29.78"W, ~92 m ASL) and a surface observation site located on the campus of UQAM (45°30′31.08″N, 73°34′07.58″W, 69 m ASL); and the observation station at the Gault Nature Reserve (Gault, 45°32'06.1"N 73°08'56.4"W, 124.95 m ASL). The YOW site was deployed by ECCC (Mariani et al., 2026) and co-located with instruments from McGill University for ECALOT, whereas the Montreal and Gault stations form part of the Adaptable Earth Observation System's (AEOS) Climate Sentinels observation network operated by McGill University and UQAM (McGill University and Université du Québec à Montréal, n.d.).

The deployed instruments at YOW are summarized in Table 2. Most instruments were fully automated and operated continuously throughout the campaign (October 2024 to March 2025). The Atmospheric Emitted Radiance Interferometer (AERI), however, was operated only under non-precipitating conditions.

https://doi.org/10.5194/egusphere-2026-5347
Preprint. Discussion started: 9 September 2026

Table 2: Surface instruments installed at the YOW surface site.

Instrument	**Measurement Principle**	**Measured Parameters**	**Notes**
		ECCC Instruments	
HALO Doppler Lidar	Coherent Doppler lidar	Attenuated aerosol backscatter profile; cloud base height; planetary boundary layer height; vertical and horizontal wind profiles; depolarization ratio	Continuous automated operation
DA10 Water Vapour Lidar	Differential absorption lidar (DIAL)	Attenuated aerosol backscatter profile; water vapour mixing ratio profile	Continuous automated operation
Micro rain radar Pro	FMCW vertically pointing radar	Hydrometeor reflectivity and fall velocity profiles; hydrometeor properties	Continuous automated operation
Pluvio^2 Rain Gauge	Weighing precipitation gauge	Precipitation amount and intensity	Continuous automated operation
Parsivel Disdrometer	Optical disdrometer	Precipitation type and intensity; particle size distribution; equivalent radar reflectivity	Continuous automated operation
FD71p Visibility and Present Weather Sensor	Optical forward-scattering sensor	Precipitation type and intensity; drop size distribution; visibility	Continuous automated operation
WXT536	Multi-parameter meteorological sensor	Pressure, temperature, relative humidity, winds, and precipitation rate	Continuous automated operation
MP3000 radiometer	Passive microwave radiometer	Temperature, humidity and water vapor profiles	Continuous automated operation
		McGill Instruments	
Atmospheric Emitted Radiance Interferometer (AERI)	Fourier-transform infrared spectrometer	Infrared spectral radiance from 520 to 3200 cm^{-1} with a spectral resolution of 0.5 cm^{-1}; Temperature and humidity retrievals capability	Not operational during precipitation events.
NR01 Net Radiometer	Broadband radiometer	Upwelling and downwelling shortwave and longwave radiative fluxes	Continuous automated operation

Detailed information on the instruments relevant to EarthCARE cal/val at the Montreal and Gault stations is summarized in Table 3.

https://doi.org/10.5194/egusphere-2026-5347
Preprint. Discussion started: 9 September 2026

Table 3: Surface instruments from the Climate Sentinels network at the Montreal and Gault stations utilized for ECALOT.

Instrument	Measurements	UQAM-Burnside Hall (Montreal)	Gault (~30 km E of Montreal)	Status
AERI	Spectrally resolved infrared radiances (containing information on temperature, humidity, clouds, and aerosols)	Y	Y	Not operational during precipitation events.
CNR4 net radiometer	Shortwave/longwave upwelling/downwelling irradiance	Y	Y	Continuous automated operation
Thermopile pyranometer	SW downwelling irradiance	N	Y	Continuous automated operation
Micro rain radar	Precipitation vertical profile	Y	Y	Continuous automated operation
Lidar Ceilometer	Cloud base and boundary layer	Y	Y	Continuous automated operation
Parsivel Disdrometer	Precipitation properties	Y	Y	Continuous automated operation
Atmospheric visibility sensor	Visibility	Y	Y	Continuous automated operation
Snow water equivalent sensor	Snow water amount	N	Y	Continuous automated operation
Tipping bucket Rain gauge	Precipitation amount	Y	Y	Continuous automated operation
Humidity, Temperature probes	Relative humidity, Temperature	Y	Y	Continuous automated operation
Snow ruler	Snow depth	N	Y	Continuous automated operation

4.3. Observational strategy

While Section 3 outlines the high-level design principles of the ECALOT campaign, their implementation required adaptation to operational constraints, including aircraft endurance, airspace restrictions, weather variability, and instrument availability. This section describes how flight timing, sampling patterns, and instrument configurations were managed to achieve the campaign objectives.

Each coordinated flight included an approximately 15-30 min underflight segment aligned with or oriented up to ~20° relative to the EarthCARE ground track (Figure 1). During the satellite overpass time, the aircraft and satellite were temporally and spatially collocated near the center of this sampling segment. The duration of the underflight segment was limited to approximately 30 min to minimize temporal and spatial mismatches. Longer underflight segments would increase temporal mismatches between the satellite and aircraft sampling progressively away from the midpoint of the segment, owing to the much slower airspeed of the Convair-580 (~100 m s^{-1}) compared to EarthCARE (~7600 m s^{-1}). These temporal mismatches further introduce uncertainty in direct comparisons due to cloud evolution and advection.

https://doi.org/10.5194/egusphere-2026-5347
Preprint. Discussion started: 9 September 2026

Since EarthCARE passes through the underflight segment in approximately 20-25 s, the aircraft heading relative to the satellite track (i.e., flying with or against the ground-track direction) has negligible impact on collocation. This provides flexibility in flight planning under constraints imposed by departure timing, weather conditions, airspace restrictions, or technical considerations.

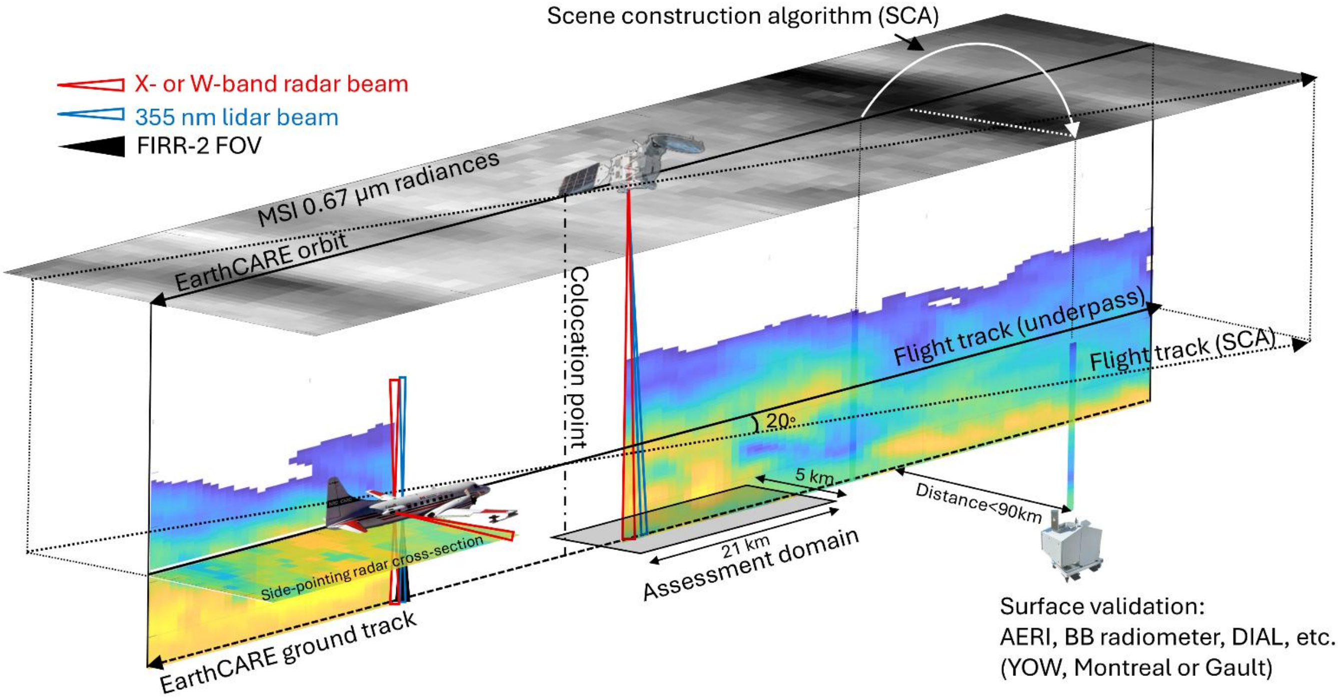

Figure 1: Schematic overview of ECALOT validation geometries involving satellite, airborne, and surface observations. This schematic does not correspond to a specific flight but illustrates the sampling geometries designed to support EarthCARE cal/val objectives.

In most cases, the underflight segment was closely aligned with the satellite ground track. During selected flights, mostly cumulus (Cu) and stratocumulus (Sc) cloud cases, the aircraft crossed the ground track at an angle of approximately 20° (Figure 1). This configuration allowed in situ sampling directly beneath the satellite at nadir near the center of the segment (colocation point), while also providing sampling of off-nadir regions immediately before and after the overpass. Such measurements support the evaluation of EarthCARE scene construction algorithm's representation of cloud structures away from the nadir track.

In addition to the underflight segment, one or two supplementary segments were typically flown in the off-nadir areas, positioned upwind and downwind of the satellite ground track. These legs sampled cloud properties at different altitudes and horizontal locations within the same cloud system, providing information on both vertical and horizontal variability. The multi-segment configuration also supports subsequent scene construction validation and Lagrangian trajectory analyses to account for atmospheric advection and temporal evolution.

https://doi.org/10.5194/egusphere-2026-5347
Preprint. Discussion started: 9 September 2026

Different flight patterns were employed depending on the sampled cloud regime. For deeper cloud systems, such as nimbostratus (Ns), level-flight segments at multiple altitudes were conducted to characterize both horizontal and vertical structure of the cloud system while maintaining stable flight conditions for NAW Doppler velocity measurements. For shallow liquid cloud regimes (e.g., Cu and Sc), porpoising and full profiling manoeuvres were incorporated during both underflight and off-nadir segments (Figure 2). These manoeuvres provided vertical profiles of liquid water content and droplet size distribution, enabling assessment of adiabatic or semi-adiabatic structure within the cloud layer.

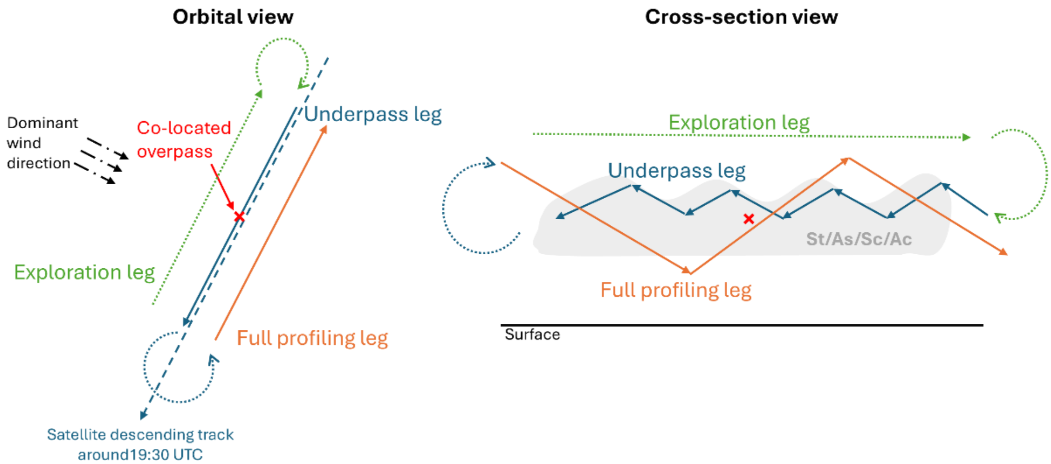

Figure 2: Porpoising and full profiling flight pattern for sampling stratiform liquid cloud layers.

Spiral profiling manoeuvres were conducted above the YOW surface site to obtain vertical profiles of atmospheric thermodynamic structure. These profiles support surface-based radiative closure assessments, provide validation of auxiliary atmospheric profiles used in the EarthCARE processing chain, and support the evaluation and calibration of Convair-580 remote sensing measurements.

In addition to the nadir- and zenith-pointing configurations of the NAW and NAX radar systems, the side-pointing beams were activated during all ECALOT flights. This configuration provides observations of the horizontal cloud cross-section extending up to approximately 10 km on the starboard side of the aircraft (Figure 1), which are valuable for evaluating the performance of the scene construction algorithm.

The AERI observations played an important role in surface-based spectral radiative closure assessments during ECALOT. When a surface site was located within the MSI swath, EarthCARE's scene construction algorithm was applied to construct atmospheric conditions above the site using EarthCARE nadir retrieval profiles (Qu et al., 2023), enabling comparison of simulated and observed spectral radiances (Figure 1). In addition, broadband net radiometers at each surface site provided complementary shortwave and longwave radiative flux measurements for broadband radiative closure assessments.

https://doi.org/10.5194/egusphere-2026-5347
Preprint. Discussion started: 9 September 2026

The Far-Infrared Radiometer-2 (FIRR-2), originally designed for ground-based observations, was modified for airborne operation and was installed on the Convair-580 during Flights 6 and 7 in the nadir-viewing port (Mariani et al., 2022). This configuration enabled airborne measurements of spectral infrared radiances, thereby extending radiative closure assessments to the aircraft level.

4.4. Summary of measurement coverage

This section summarizes the overall spatial and temporal coverage of the ECALOT campaign. Figure 3 provides an overview of the ECALOT sampling domain, including the EarthCARE ground-track within 350 km to YOW during the campaign period (blue lines), the primary airborne sampling region for each flight (black rectangles), and the locations of the surface sites (coloured dots).

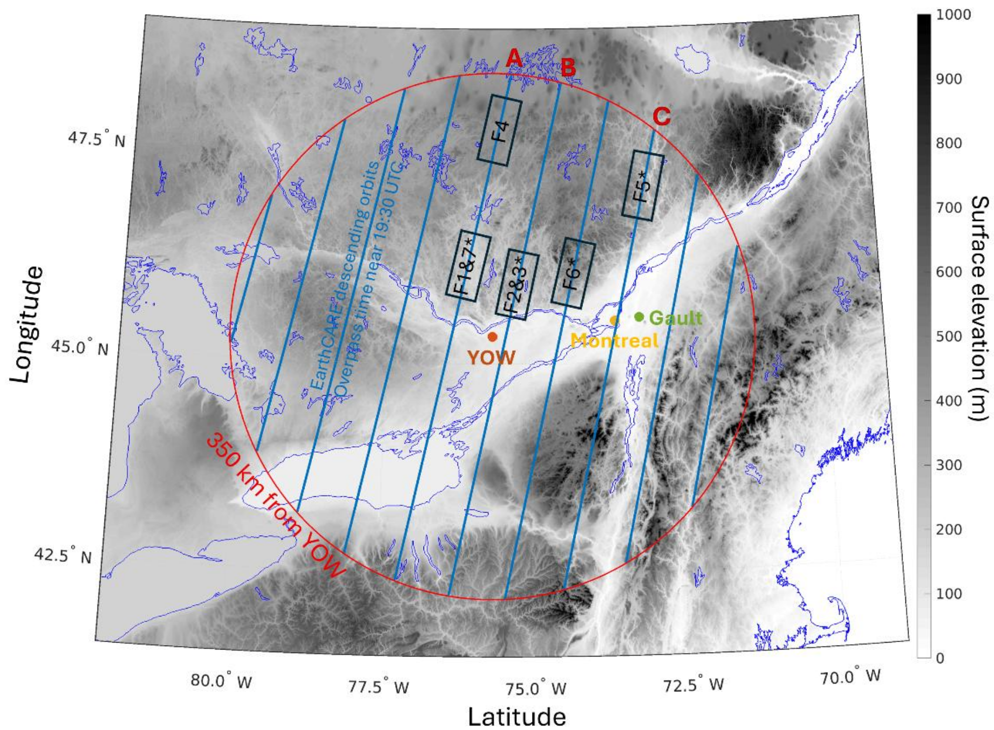

Figure 3: EarthCARE descending overpasses (blue lines) and the ECALOT airborne sampling regions during each satellite overpass (black rectangles). Flight identifiers (F1, F2, etc.) correspond to individual research flights. An asterisk (*) following the flight number indicates that ice or mixed-phase cloud conditions were encountered, whereas flights without an asterisk were predominantly characterized by liquid clouds. The locations of the three surface-based observation sites are also shown. The recurrent EarthCARE orbits labelled A, B, and C provide MSI swath coverage over the surface sites and can therefore be used for surface-based radiative closure assessments.

In total, seven research flights were conducted between 1 October 2024 and 25 March 2025. A summary of the flights is provided in Table 4. While all flights were designed to support EarthCARE's cloud retrieval cal/val, Flight 1 and 2 also targeted atmospheric conditions with aerosol layers associated with wildfire activity in Canada during the warmer season.

https://doi.org/10.5194/egusphere-2026-5347
Preprint. Discussion started: 9 September 2026

Instrument configurations also varied across flights. The FIRR-2 instrument was installed in the nadir port of the Convair-580 during two flights (Flight 6-7), replacing the AECL nadir-viewing lidar. This configuration enabled additional aircraft-based infrared radiative closure measurements. The HiSRAMS instrument was available during Flights 1-3 and 6-7, providing temperature and humidity profile measurements that support evaluation of EarthCARE auxiliary atmospheric fields and provide additional constraints for cloud physics and radiative closure analyses.

Table 4: Summary of the ECALOT flights. For detailed region for each flight, please refer to Figure 3.

Flight ID	Date (UTC)	Time (UTC)	Region	Target	EarthCARE Frame
1	1 Oct. 2024	18:23 - 20:20	Northwest of Ottawa	Liquid clouds (Cu/Sc) and aerosols	01598D
2	10 Oct. 2024	18:00 - 20:35	Northeast of Ottawa	Liquid clouds (Cu/Sc) and aerosols	02098D
3	4 Nov. 2024	18:00 - 21:15	Northeast of Ottawa	Ice, mixed-phase clouds, rain (Ns)	02487D
4	20 Nov. 2024	18:00 - 21:15	North of Ottawa	Liquid clouds (Sc)	02736D
5	22 Nov. 2024	17:30 - 21:10	North of Montreal	Ice, mixed-phase clouds (Ns)	02767D
6	27 Jan. 2025	17:50 - 21:50	Northwest of Montreal	Ice clouds (Ns)	03794D
7	25 Mar. 2025	18:28 - 20:55	Northwest of Ottawa	Ice, mixed-phase clouds (Ns)	04681D

Surface sites provided continuous background measurements throughout the campaign period. As shown in Figure 3, the airborne sampling regions during most overpass events were spatially separated from the surface site locations, except for Flights 2 and 3. This separation resulted from constraints including the geographic locations of EarthCARE ground tracks, airspace restrictions near major urban areas (e.g., the orbit during Flight 5 passed through Montreal), and spatial differences between the targeted cloud systems and the surface site locations. Nevertheless, the surface sites provide independent validation opportunities during recurrent orbit overpasses when no coordinated flight was conducted, thereby extending the temporal coverage of calibration and validation activities beyond the airborne sampling periods. Additionally, the recurrent EarthCARE orbits labelled A, B, and C pass sufficiently close to the surface sites to ensure MSI swath coverage. This allows the application of the scene construction algorithm to reconstruct atmospheric conditions above the surface sites, bridging the spatial separation between the satellite ground track and ground-based observations. The surface measurements therefore provide extended opportunities to calibrate and validate EarthCARE's retrievals of precipitation amount, type and cloud base height through direct comparisons with surface observations, and cloud properties through surface-based radiative closure assessments.

https://doi.org/10.5194/egusphere-2026-5347
Preprint. Discussion started: 9 September 2026

5. Dataset overview and quality control

5.1. Overview of ECALOT Data Products

ECALOT data are archived as instrument-specific datasets organized by platform and, for airborne observations, by flight. All datasets are time-stamped in Coordinated Universal Time (UTC) and include geolocation information. Although the archive retains this instrument-based structure, Table 5 provides a functional mapping between ECALOT measurements and the EarthCARE processing chain. For conciseness, the measurements are grouped into broad observational domains rather than listed as individual variables.

Table 5: Summary of ECALOT datasets and their relevance to EarthCARE Level 1 and Level 2 products.

ECALOT Measurement Domain	Validation/Comparison Domain	EarthCARE Product Level & Type
	Airborne measurements	
Airborne W-band radar profiles (zenith, nadir & side)	Reflectivity Doppler velocity Vertical cloud and precipitation structure Cross-track structural characterization (side-pointing geometry)	Level 1 calibrated CPR reflectivity and Doppler velocity profiles Level 2 processed radar reflectivity and Doppler velocity profiles Level 2 scene construction products (3D structural consistency)
Airborne 355 nm lidar profiles (zenith & nadir)	Backscatter and depolarization properties Extinction and layer structure Cloud phase discrimination and aerosol-cloud separation	Level 1 calibrated backscatter profiles Level 2 ATLID backscatter, depolarization and extinction products Level 2 ATLID target classification
In situ cloud microphysics probes	Bulk cloud water content (ice and liquid) Number concentration, size distribution, and effective radius Cloud phase and particle habits Sampling in nadir and off-nadir regions	Level 2 cloud microphysical retrieval products (single-instrument, composite, synergy) Level 2 scene construction products (off-nadir sampling)
In situ aerosol probes	Aerosol size distribution Aerosol layer characterization	Level 2 ATLID/synergy target classification Level 2 aerosol extinction product
Atmospheric state probes	Temperature and humidity profiles Wind measurements at aircraft level	Level 1 auxiliary meteorological inputs Level 2 cloud retrieval products (through thermodynamic constraint)
Airborne far-infrared radiometer	Upwelling spectral far-infrared radiance Radiative closure at aircraft level	Level 2 radiative flux and heating-rate products Level 2 cloud retrieval products (via radiative closure assessment)

https://doi.org/10.5194/egusphere-2026-5347
Preprint. Discussion started: 9 September 2026

	Surface measurements	
Surface radiation instruments	Surface shortwave and longwave radiative fluxes Downwelling spectral infrared radiance Surface-level radiative closure	Level 2 radiative flux and heating-rate products Level 2 cloud retrieval products (via surface radiative closure assessment)
Surface lidars	Water vapor profiles Aerosol and cloud layer structure (including cloud base height) Wind measurements	Level 1 auxiliary meteorological inputs (humidity and wind) Level 2 target classification products
Surface microwave radiometer	Temperature and humidity profiles	Level 1 auxiliary meteorological inputs (temperature and humidity)
Surface weather sensors	Precipitation amount and type Surface weather conditions	Level 2 target classification products Level 2 precipitation and hydrometeor retrieval products

5.2. Quality Control and Screening Procedures

The quality control (QC) procedures were applied to all ECALOT measurements prior to archiving to ensure calibration accuracy and internal consistency. These procedures were conducted at the instrument level and focused on identifying data anomalies and signal artifacts and removing non-physical or instrument-contaminated measurements.

5.2.1. Airborne active remote sensing measurements

5.2.1.1 Airborne radars

Airborne radar observations were collected using the NRC airborne W- and X-band radar system (NAWX) and the ECCC K-band Precipitation Radar (KPR). The NAWX antennas are housed within an unpressurized blister radome mounted on the right side of the aircraft fuselage, while the KPR antenna was installed on the left wingtip pylon. For NAWX, data are available from three viewing directions (zenith, nadir, and side-looking), whereas the KPR provides observations only in the zenith- and nadir-looking directions. Key radar parameters are summarized in Table 6. More detailed descriptions of the NAWX and KPR systems can be found in Wolde and Pazmany (2005) and Haimov et al. (2018), respectively. For the ECALOT campaign, the radar complex in-phase (I) and quadrature (Q) samples were processed into power measurements and complex pulse-pair products according to the radar system specifications. These products were subsequently recorded in binary format for further processing and analysis.

The end-to-end calibration for NAWX nadir antennas was done using backscattering properties of the water surface (Li et al., 2005). For 94 GHz radars at an incidence angle of 10°, the mean value of normalized radar cross section (σ^0) in clear air conditions is 5.85 dB with a standard deviation of 0.6 dB (Li et al., 2005). Calibration for other NAWX antennas and KPR is

https://doi.org/10.5194/egusphere-2026-5347
Preprint. Discussion started: 9 September 2026

done by comparing measurements between antenna ports. More details on calibration and results for NAWX and KPR radars are described in Wolde et al. (2019) and Nguyen and Wolde (2021).

Table 6: Radar parameters for the ECALOT campaign.

Parameter	W-band	Ka-band	X-band
RF output frequency	94.05 GHz	35.64 GHz	9.41 GHz ± 30 MHz
Nadir/Zenith antenna beamwidth	0.75	4.2	4.5°
Pulse width	500 ns	0.25 µs/2.5 µs (short pulse/chirp)	500 ns
Range resolution	75 m	30 m, 60 m	75 m
Dwell time	0.14 s	0.2 s	0.23 s
Sampling resolution	34.26 m	30 m	30 m

5.2.1.2 Airborne lidars

The Airborne Elastic Cloud Lidar (AECL) is a compact 355 nm airborne lidar that provides atmospheric profiles up to approximately 5 km with 1.5 m range resolution and 20 Hz temporal resolution (Baibakov et al, 2016). The instrument measures both co-polarized and cross-polarized return signals, allowing particle depolarization to be estimated. Two AECL systems were installed on the Convair-580, with one pointing nadir and the other pointing zenith.

AECL data from the four measurement channels were processed using a standard quality-control workflow. Profiles were height-aligned using the ground-spike method (Newsom et al., 2017), saturated points were flagged, and the recorder baseline was removed. Detector-response corrections were applied using a non-linear deadtime correction (Donovan, 1993), followed by co-averaging, background subtraction, and dark-count correction.

For each polarization component, low- and high-gain channels were merged into a single profile. The low-gain signal was scaled to match the high-gain signal in the linear range, following established signal-gluing methods (Newsom et al., 2017). The merged profile primarily used the high-gain data. Where the high-gain channel was saturated or missing, it was replaced by the corresponding low-gain signal.

5.2.2. In situ measurements

Quality control of Optical Array Probes (OAP) 2DS and HVPS-3/4 measurements was conducted to identify and eliminate artifacts arising from particle shattering, splashing, diffraction effects, and optical contamination. Shattering artifacts were addressed using frame-based methods (Korolev and Isaac, 2005) and inter-arrival-time algorithms (Field et al., 2006). Procedures for recovering valid, partially imaged particles affected by diffraction or multi-branched structures followed the approach of Korolev and Field (2015). Periods impacted by optical fogging or melted shed water were flagged and excluded from the archived, quality-controlled datasets.

https://doi.org/10.5194/egusphere-2026-5347
Preprint. Discussion started: 9 September 2026

Additional considerations relate to uncertainties associated with sample-area definition, diffraction effects and elevated shattering contamination, particularly for particles smaller than approximately 100 µm, for which concentration estimates are subject to larger relative uncertainty (Korolev et al., 1998). The uncertainty in derived bulk quantities, such as ice water content (IWC) and extinction, is estimated to be on the order of 20-40%, consistent with established assessments.

Scattering probe data (FCDP and CDP) were corrected for particle coincidence effects and screened to exclude periods affected by optical contamination (such as fogging or icing) and non-nominal instrument operation. Special attention was devoted to sample-area stability and size-bin threshold definitions, as these factors directly influence estimates of droplet number concentration, extinction, and LWC. For properly functioning probes, the uncertainty in droplet concentration is approximately 20%, while uncertainties in extinction and liquid water content are typically between 20-40%. Liquid water content calculated from scattering probes was validated against measurements from two Nevzorov probes. Time segments with CDP and FCDP exhibiting large discrepancies in LWC, measured by the Nevzorov probes, were flagged and excluded from analysis.

Nevzorov liquid and total water content measurements were corrected for clear-sky zero offsets using polynomial regression incorporating true airspeed, pressure, temperature, and reference sensor power during cloud-free periods. The residual clear-sky offset typically was generally less than 0.005 g m^{-3} within individual flights.

Bulk liquid and ice water contents were calculated using established correction procedures accounting for sensor collection efficiency and thermodynamic effects (Korolev et al., 1998; Korolev and Strapp, 2002). In the ice water content calculations, a rebound fraction of 40% of ice mass from the TWC sensor was assumed. Uncertainty in liquid water content for pure liquid clouds is generally within ~20%, but increases in mixed-phase or precipitation conditions. Ice water content uncertainties depend on particle size and habit and potentially reaching 50% or higher in ice clouds, with larger uncertainty possible in mixed-phase environments.

No geophysical filtering or matchup-based screening was imposed at the archiving stage; such criteria are analysis-dependent and may be applied by users according to their specific scientific objectives.

5.2.3. Airborne radiation measurements

FIRR-2 measurements were calibrated using onboard hot and ambient black bodies sandwiching each acquisition cycle. Calibrated radiances were synchronized with aircraft navigation data (latitude, longitude, and altitude) for all the flight segments. Periods prior to take-off, dedicated to the hot black body preheating, were excluded from the archived datasets. Additional post-processing is required to remove the radiative impact of the protective diamond window installed in the instrument's field of view (FOV); its transmittance, reflectance and emittance characteristics have been characterized and their influence on measured radiances is being accounted for.

5.2.4. Surface measurements

The datasets collected by the suite of ECCC instruments underwent automated QC and quality assurance (QA) procedures throughout the entire ECALOT campaign. A comprehensive summary of the instruments, their configuration, precision and uncertainty, the processing, and the QC applied is provided in Tables A1-A7 in Mariani et al. (2024). The automated algorithms were designed to remove outliers; for the surface meteorological observations (Pluvio2, Parsivel, FD71P, and WXT520), measurements that fell outside of the 3-sigma normal climatological range were rejected, as were those exhibiting rates of change greater than seasonal-dependent thresholds (e.g., >20 hPa h^{-1} change).

An automated QC algorithm based on the lidar signal to noise ratio, as described in Mariani et al. (2018), was used to QC all Doppler lidar data. In the case of post-processed products, such as the retrieved cloud base height and planetary boundary layer height from the Doppler lidar, no additional QC was performed and their uncertainties are estimated to be ±10 m and ±120 m, respectively. The DA10 observations were quality-controlled using the Vaisala software's estimation of maximum range and uncertainty, as described in Mariani et al. (2021). Similarly, QC flags provided by Radiometric's MP3000 software were used to QC the level 2 radiometer-retrieved thermodynamic profiles. No additional QC was performed on the micro rain radar dataset; observations were manually quality-controlled on a case-by-case basis.

The AERI measurements were processed to ensure spectral consistency and robust QC. Measurement uncertainty was quantified using two metrics: absolute radiometric calibration uncertainty, derived as the 1% (3σ) of the ambient blackbody apex radiance (Knuteson et al., 2004), and instrument noise, characterized by the noise equivalent spectral radiance. Additionally, comprehensive quality assurance was integrated by extracting 25 specific operational and environmental flags from the AERI Armory software, allowing for the precise identification and removal of degraded or non-physical spectra.

For the net radiometers, data underwent physical corrections and quality control to remove instrumental artifacts. Longwave radiation measurements were first corrected for sensor thermal emission using the internal sensor temperature and the Stefan-Boltzmann law. Finally, threshold-based filters removed non-physical outliers: incoming shortwave values below -5 W m^{-2} were rejected and replaced with fill values, while minor negative shortwave values (-5 to 0 W m^{-2}) attributed to sensor noise were zeroed.

5.3. GEOMS data format

Following QC and QA procedures, ECALOT datasets were converted into GEOMS-compliant data products to ensure interoperability, traceability, and long-term accessibility. The GEOMS (Generic Earth Observation Metadata Standard) convention (De Mazière et al., 2018) provides a standardized structure for geophysical variables, metadata documentation, and quality flags, facilitating integration with satellite validation archives and international calibration and validation frameworks. For ECALOT, each dataset was reformatted to include standardized variable naming conventions, consistent units, uncertainty descriptors, and platform-specific geolocation information.

https://doi.org/10.5194/egusphere-2026-5347
Preprint. Discussion started: 9 September 2026

Conversion of ECALOT datasets to the GEOMS format requires compliance with standardized file structures and metadata conventions. Data were organized by instrument or measurement category, with each dataset following the corresponding GEOMS template that defines its structure and metadata requirements. New GEOMS templates were developed for instruments not previously represented in the framework, while existing templates were updated where necessary to accommodate additional variables relevant to EarthCARE cal/val.

6. EarthCARE cal/val and science applications

Using an end-to-end approach, the ECALOT campaign aims to support the cal/val of EarthCARE products ranging from Level 1b to Level 2b (Table **7**). In addition, the vertically and horizontally resolved observations provide valuable information for evaluating cloud representation in NWP models. The following subsections highlight selected aspects of this relevance.

Table 7: List of relevant EarthCARE products to be validated using ECALOT observations.

Product Name	Level	Description
C-NOM	1b	CPR received echo power, reflectivity factor and Doppler velocity profiles
A-NOM	1b	ATLID Calibrated attenuated backscatter
X-MET	1d	Auxiliary meteorological/surface data based on IFS model outputs
C-CD	2a	CPR corrected Doppler velocity
C-FMR	2a	CPR feature mask and corrected reflectivity
C-CLD	2a	CPR retrievals of cloud and precipitation properties
C-TC	2a	CPR based target classification for cloud and precipitation
M-COP	2a	MSI retrievals of vertically integrated cloud properties, including optical depth and water path
A-EBD	2a	ATLID processed extinction, backscatter and depolarization
A-AER	2a	ATLID aerosol profiles
A-ALD	2a	ATLID aerosol layer descriptor
A-ICE	2a	ATLID retrievals of ice water content and effective radius
A-TC	2a	ATLID based target classification for cloud and aerosols
AC-TC	2b	Synergistic target classification for cloud and aerosols
ACM-CAP	2b	Synergistic retrievals of cloud and aerosols
BMA-FLX	2b	BBR based SW and LW fluxes with 3 views (forward, nadir and backward)
ACM-COM	2b	Composite product of cloud and aerosols based on single-instrument retrievals, and auxiliary inputs
ACMB-3D	2b	3D scene construction algorithm
ACM-RT	2b	Radiative transfer simulation using both single column approximation and 3D Monte Carlo method
ACMB-DF	2b	Radiative closure assessment

6.1. Airborne active remote sensing comparisons

6.1.1. Radar validation

Radar validation during ECALOT focuses on direct comparison between the data products of CPR aboard EarthCARE and the NAW radar on the Convair-580 aircraft. The comparison is conducted between CPR's reflectivity and Doppler velocity profiles observed from space (C-NOM, C-CD, C-FMR) and the corresponding NAW observations obtained from both zenith-

https://doi.org/10.5194/egusphere-2026-5347
Preprint. Discussion started: 9 September 2026

and nadir-pointing beams under coordinated underflight conditions. Coordinated satellite overpasses and aircraft underflights were therefore required to minimize temporal and spatial offsets, enabling meaningful comparison of reflectivity and Doppler velocity within approximately collocated cloud volumes.

To achieve accurate cross-comparison between EarthCARE CPR Level 1 and Level 2 products and the NAW radar observations, the NAW observations must first be re-gridded to the CPR volume, such that the horizontal and vertical resolutions closely match each other. The radar volume-matching procedure consists of the following two steps:

- Range-axis alignment: airborne radar observations are projected onto the vertical axis at the aircraft location using aircraft Inertial Measurement Unit (IMU) measurements to account for aircraft's rotation variations, e.g., changes in pitch, roll, and heading angles. The observations are then aligned with the CPR's range coordinate using the ground return as a reference.
- Re-gridding: the aligned radar observations are then re-gridded to minimize the effects of differences along track and vertical sampling resolution between the two radar systems. Thus, the high-resolution NAW data is gridded onto coarser CPR resolution following a distance-weighted average. Figure **4** below shows an example of this comparison between CPR (C-FMR, Baseline BC) and NAW reflectivity for Flight 5 on Nov 22, 2025.

Good agreement was found between the Level 2 radar reflectivity product (C-FMR) and the corresponding NAW measurements during Flight 5, with a coefficient of determination (R^2) greater than 0.96. The data gap near the center of the underflight segment in Figure 4b and Figure 4c is partly due to the NAW radar being turned off near the closest collocation with EarthCARE to avoid interference with the CPR and to high roll angles from the Convair-580 to remain near the central part of the EarthCARE orbit (Figure 4a). This latter factor makes the comparison less reliable in that part of the segment, consequently it was excluded from the analysis. Similar agreement was found for the other nimbostratus cases (not shown). Doppler velocity comparisons were also performed for selected nimbostratus cases. A more detailed evaluation will be presented in a dedicated study.

https://doi.org/10.5194/egusphere-2026-5347
Preprint. Discussion started: 9 September 2026

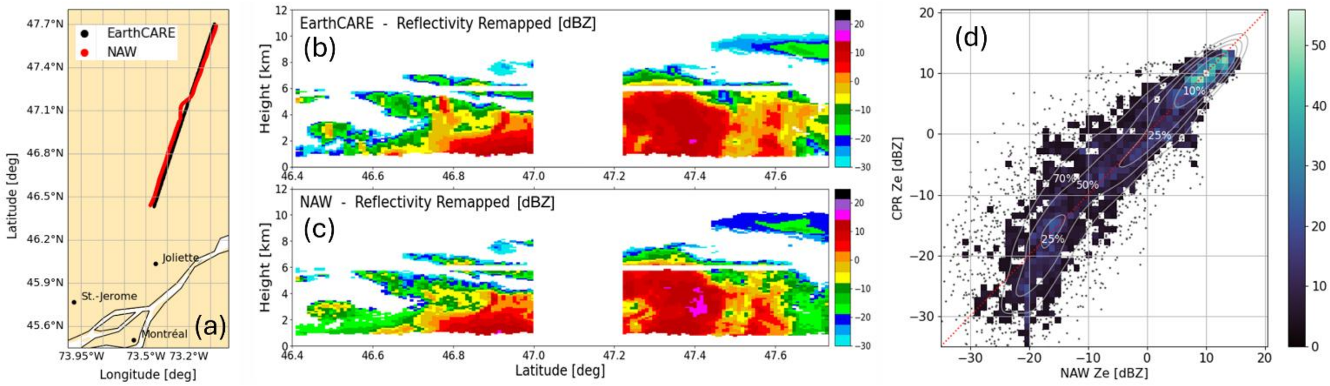

Figure 4: (a). Underflight segment of ECALOT Flight 5. (b). Radar reflectivity from EarthCARE (C-FMR, Baseline BC). (c). Radar reflectivity from NAW. (d). heatmap of CPR reflectivity [Ze - dBZ] vs NAW reflectivity [Ze - dBZ] (shaded), the white contours show the enclosed percentage frequency and the red dotted line represents the 1:1 line.

6.1.2. Lidar validation

Lidar validation during ECALOT involves comparison between ATLID aboard EarthCARE and the AECL lidars on the Convair-580 aircraft. Because both systems operate at 355 nm, comparisons of attenuated backscatter profiles (A-NOM, A-EBD) provide a consistent basis for evaluating signal magnitude and vertical layer structure.

In addition to total backscatter, comparisons include co-polar and cross-polar components, enabling assessment of depolarization ratio and phase discrimination performance (A-NOM, A-EBD). These quantities are particularly relevant for evaluating cloud phase in stratiform cloud systems. Airborne lidar measurements were obtained in zenith-pointing configuration throughout the campaign, while nadir-pointing observations were available during the first five flights. The coordinated underflight geometry enables comparison of ATLID spaceborne profiles with approximately collocated airborne observations.

6.2. Ice cloud property retrievals

EarthCARE provides an unprecedented opportunity to probe the dynamical structure of clouds. The combined use of radar, lidar, and multispectral imager measurements offers complementary constraints for retrieving cloud properties. In particular, the Doppler capability of CPR provides additional information on the terminal fall speed of ice particles, thereby enhancing the retrieval quality of ice cloud microphysical properties. However, accurate separation of Doppler velocity (v_d) into vertical air motion (v_w) and particle terminal fall speed (v_t) is critical.

At the time of launch, particle terminal fall speed v_t was retrieved using a simplified neighborhood-averaging approach based on the general framework of Protat and Williams (2011). Doppler velocity v_d samples were grouped into 3-dBZ reflectivity bins within a small vertical neighborhood and over a sequence of along-track averaging windows ranging from 10 to 40 km.

https://doi.org/10.5194/egusphere-2026-5347
Preprint. Discussion started: 9 September 2026

The method aimed to suppress v_w and measurement noise (ϵ), averaging out their contributions, which are assumed to have zero mean within the sampling domain, while retaining the most spatially representative estimate of v_t. While this approach provides a practical estimate of v_t, the retrieval depends on the size of the spatial averaging domain under certain conditions. In particular, averaging Doppler velocity over different spatial scales can lead to variations in the inferred v_t, especially in scenes with strong along-track variability in cloud structure and dynamics, such as those influenced by gravity waves with wavelengths comparable to the averaging window (10-40 km). Under such conditions, the assumption that vertical air motion contributions average out within the sampling volume may not hold, leading to increased uncertainty in separating v_d into v_t and v_w.

A specific case was observed during ECALOT Flight 6 on 27 January 2025 (Frame 03794D), during which the gravity wave pattern was observed through the CPR observation (alternative positive and negative v_d near the flight altitude in Figure 5c), and through Convair-580's measurements of v_w (black line in Figure 5d). The correlation between v_w and v_d at the flight altitude (blue line in Figure 5d) is clear near the aircraft-satellite collocation point (black dashed line in Figure 5d). In practice, the true vertical wind might not average out to zero over a distance smaller than 40 km, which could negatively impact on the accuracy of estimated v_t. Moreover, the retrieval uncertainty could exceed the geophysical variability within these relatively short averaging windows. The airborne observations from ECALOT therefore provide independent constraints on v_t (derived from ice particle size distributions) and v_w (Hogan et al, 2026). These findings motivated the development of an adaptive weighted-averaging approach that jointly constrains reflectivity, temperature, spatial proximity, measurement uncertainty, and signal resolvability. The updated algorithm considers substantially larger candidate windows (100–250 km for ice and snow and 20–100 km for rain) and selects the averaging scale independently for each radar gate to balance statistical precision and local representativeness (Puigdomènech Treserras et al., 2026).

Moreover, both ECALOT Flight 3 on November 4, 2024 (Frame 02487D) and Flight 6 have been used to evaluate the ice-cloud retrievals of both the radar-only C-CLD product and the synergistic ACM-CAP product (Hogan et al., 2026). These comparisons demonstrated a good retrieval of ice water content from both C-CLD and ACM-CAP, but a tendency for ACM-CAP to underestimate ice effective radius by 15-25%. They also highlighted the challenge of making a reasonable retrieval of ice density. These results are being used to inform the further development of these algorithms.

https://doi.org/10.5194/egusphere-2026-5347
Preprint. Discussion started: 9 September 2026

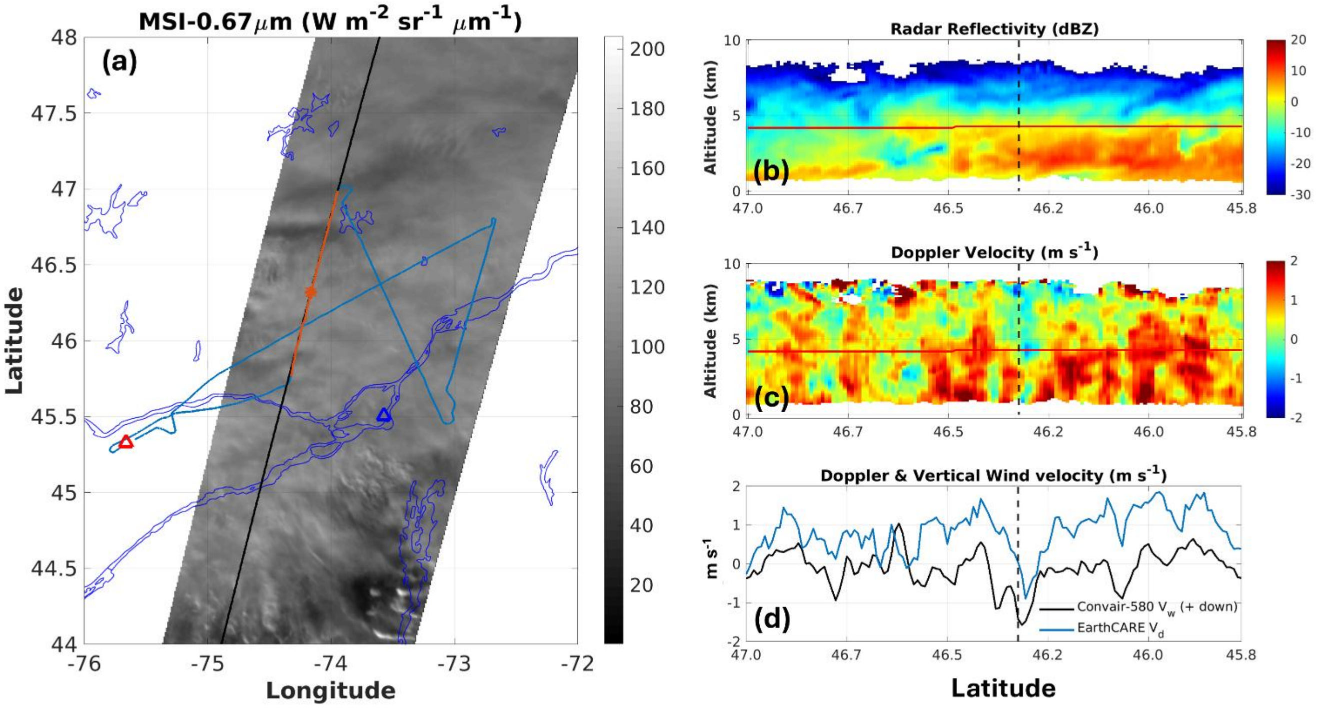

Figure 5. Radar reflectivity, Doppler velocity and vertical wind during ECALOT Flight 6 for the cal/val of EarthCARE frame 03794D. All EarthCARE products used are from the Baseline BA. (a). MSI 0.67 µm TOA radiances during the underflight segment (red line) of ECALOT Flight 6. Red asterisk: satellite-aircraft collocation point, red triangle: Ottawa surface site, blue triangle: Montreal surface site. (b). CPR radar reflectivity (C-FMR) on the underflight section. Red line: aircraft flight altitudes. Dashed line: aircraft-satellite collocation point. (c). similar to (b) but for Doppler velocity from C-CD product. (d). Doppler velocity at the flight altitude (blue line) from C-CD and Convair-580 observed vertical wind velocity (positive sign: downward).

6.3. Liquid cloud validation & porpoising flight

Liquid clouds, such as stratocumulus, are prevalent and can persistently cover large regions of the Earth's surface. They involve a range of interacting physical processes, including boundary-layer dynamics, cloud microphysical processes, radiative heating and cooling, etc. Improved representation of these clouds through EarthCARE observations can enhance our understanding of these processes and contribute to their improved representation in weather and climate models.

However, retrieving the vertical structure of stratocumulus clouds remains challenging. Because liquid cloud droplets are small, CPR may not retrieve all liquid cloud layers (C-CLD), particularly when clouds have low liquid water content and small droplet sizes. In contrast, ATLID can retrieve thin ice clouds effectively (A-ICE), but its signal is rapidly attenuated in the presence of liquid clouds, limiting its ability to probe cloud interiors. In addition, liquid water path retrieved from MSI (M-COP) represents a vertically integrated quantity and does not provide information on the vertical distribution of liquid water. As a result, the combined CPR-ATLID-MSI observations, whether used in composite (ACM-COM) or synergistic (ACM-CAP) retrieval approaches, may provide limited constraints on the vertical variation of liquid cloud properties.

https://doi.org/10.5194/egusphere-2026-5347
Preprint. Discussion started: 9 September 2026

To better constrain liquid cloud vertical structure, in situ observations are required. During ECALOT, porpoising and full profiling manoeuvres were employed to sample the vertical variation of liquid cloud properties during Flights 1, 2 and 4. These manoeuvres provide detailed vertical variations that can be used to assess the representativeness of remotely sensed retrievals and to examine whether observed liquid cloud layers follow adiabatic or semi-adiabatic vertical profiles.

An example is shown in Figure 6 from ECALOT Flight 4, during which a two-layer stratocumulus cloud system was observed, with one layer near ~900 m ASL altitude and another near 3 km ASL. Porpoising flights were conducted along the highlighted flight segment (red line in panel a of Figure 6), with the variation in flight altitude shown in panel (b). The two-dimensional (2D) histograms in panels (c) and (d) for LWC and liquid effective radius exhibit clear adiabatic behaviour (adiabatic profile shown in Figure 6c). These observations provide valuable constraints for evaluating and improving liquid cloud retrieval algorithms used in EarthCARE.

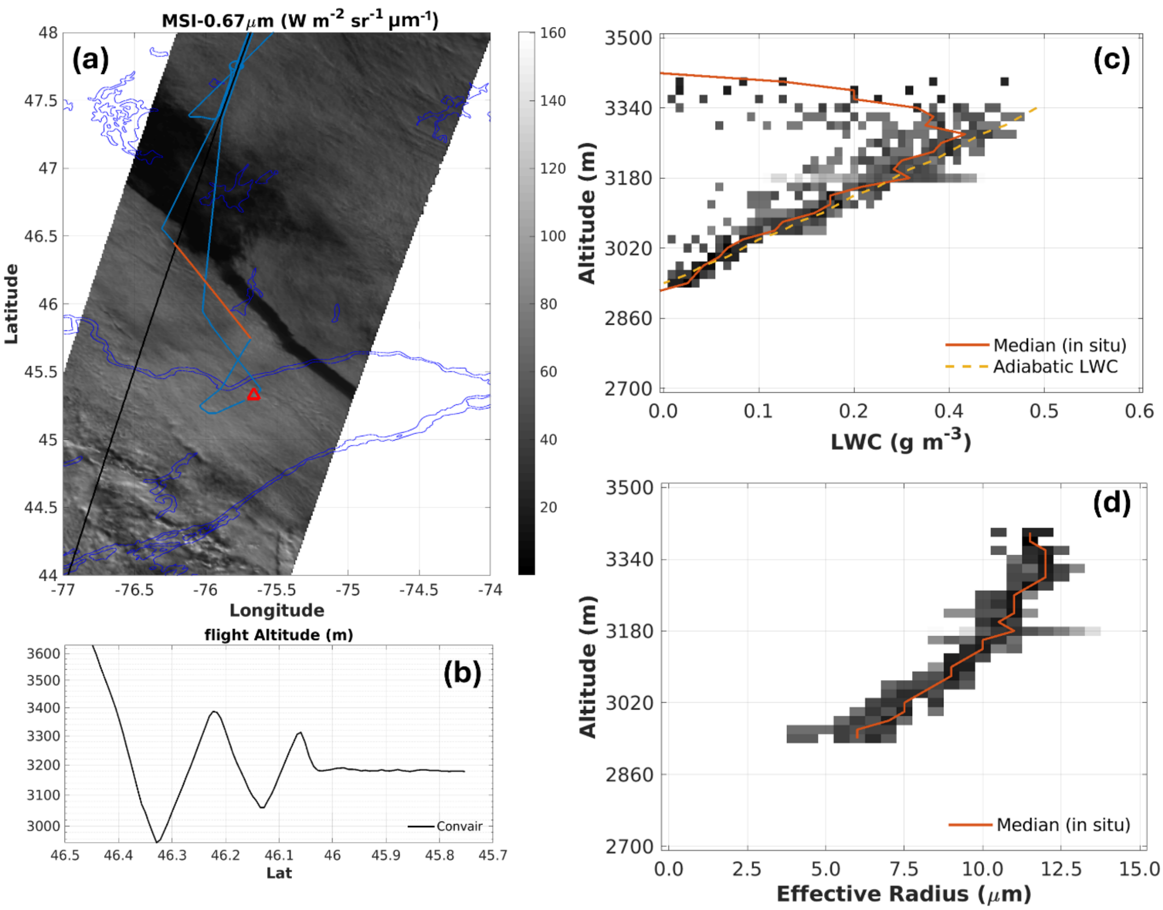

Figure 6: Porpoising flight during Flight 4 to sample vertical variation of liquid cloud layer. The corresponding EarthCARE frame is 02736D. (a). MSI 0.67 µm spectral radiances. Black line: EarthCARE ground track, blue line: Convair-580 flight track, red line: selected segment with porpoising manoeuvre. (b). flight altitudes for the selection flight segment. (c). 2D histogram of LWC from in situ observations with

https://doi.org/10.5194/egusphere-2026-5347
Preprint. Discussion started: 9 September 2026

red line representing the median values at each altitude bin and dashed orange line representing the adiabatic profile of LWC. (d). same as (c) but for liquid effective radius.

6.4. Scene construction validation

The scene construction algorithm (ACMB-3D) plays an important role in EarthCARE radiative closure assessment (ACMB-DF). It is responsible for constructing the 3D atmospheric scene in the off-nadir region, as the radiative closure assessment domain spans a 5 × 21 pixel area (Figure 1), comprising five across-track pixels (the nadir pixel plus two off-nadir pixels on each side) and twenty-one pixels along track (1 pixel ≈ 1 km). In addition, 3D radiative transfer simulations require surrounding buffer zones beyond the assessment domain, typically extending to the 7th across-track pixel (approximately 7 km). Consequently, the quality of the ACMB-3D scene construction has a direct impact on the accuracy of radiative closure assessments.

Previous evaluations of the scene construction algorithm have relied on high-resolution NWP model simulations (Barker et al., 2021; Qu et al., 2023). The advantage of this approach is that the 3D cloud field is fully known, facilitating controlled evaluation. However, even at high resolution, fine-scale cloud structures are not always well represented by the numerical models, particularly with respect to vertical structure, microphysical properties, and mixed-phase processes. Evaluation of the scene construction algorithm under real atmospheric conditions therefore provides a more realistic assessment of its performance.

Two complementary approaches were implemented during ECALOT to evaluate the performance of the ACMB-3D product. The first approach makes use of in situ observations collected in stratocumulus cloud conditions. During Flights 2 and 4, the Convair-580 underflight tracks were designed to cross the satellite ground track at an angle of approximately 20°, with the satellite overpass occurring when the aircraft was located on the nadir track (Figure 1). This flight geometry enables collocated in situ sampling at nadir while also sampling off-nadir regions shortly before and after the overpass. These measurements provide valuable information for assessing how well the scene construction algorithm represents cloud structure away from nadir (Qu et al., 2026).

The second approach uses observations from the Convair-580 starboard-side-pointing W-band radar to evaluate scene construction performance in deeper cloud systems, such as nimbostratus clouds (Figure 1). The side-pointing radar provides measurements extending up to approximately 10 km from the aircraft, covering the spatial range most relevant for scene construction in radiative closure assessment. This approach provides continuous sampling of off-nadir cloud structure without interfering with nadir- or zenith-pointing remote sensing or in situ measurements along the satellite ground track (Qu et al., 2026). It is therefore well suited for evaluating the 3D cloud fields generated by ACMB-3D.

Figure 7 shows an example from Flight 6 on 27 January 2025 for a nimbostratus case, comparing the NAW side-looking radar reflectivity (panel d) with the constructed side-looking reflectivity (panel e). The construction uses the ACMB-3D construction index (baseline configuration, BC), with the Convair-580 zenith- and nadir-pointing radar reflectivity serving as the nadir

https://doi.org/10.5194/egusphere-2026-5347
Preprint. Discussion started: 9 September 2026

source (panel c). A similar comparison can be performed using EarthCARE CPR reflectivity as the nadir source and the conclusion is similar (not shown). The observed and constructed side-looking reflectivities show strong agreement, indicating good performance of the scene construction. A more detailed analysis is presented in Qu et al. (2026).

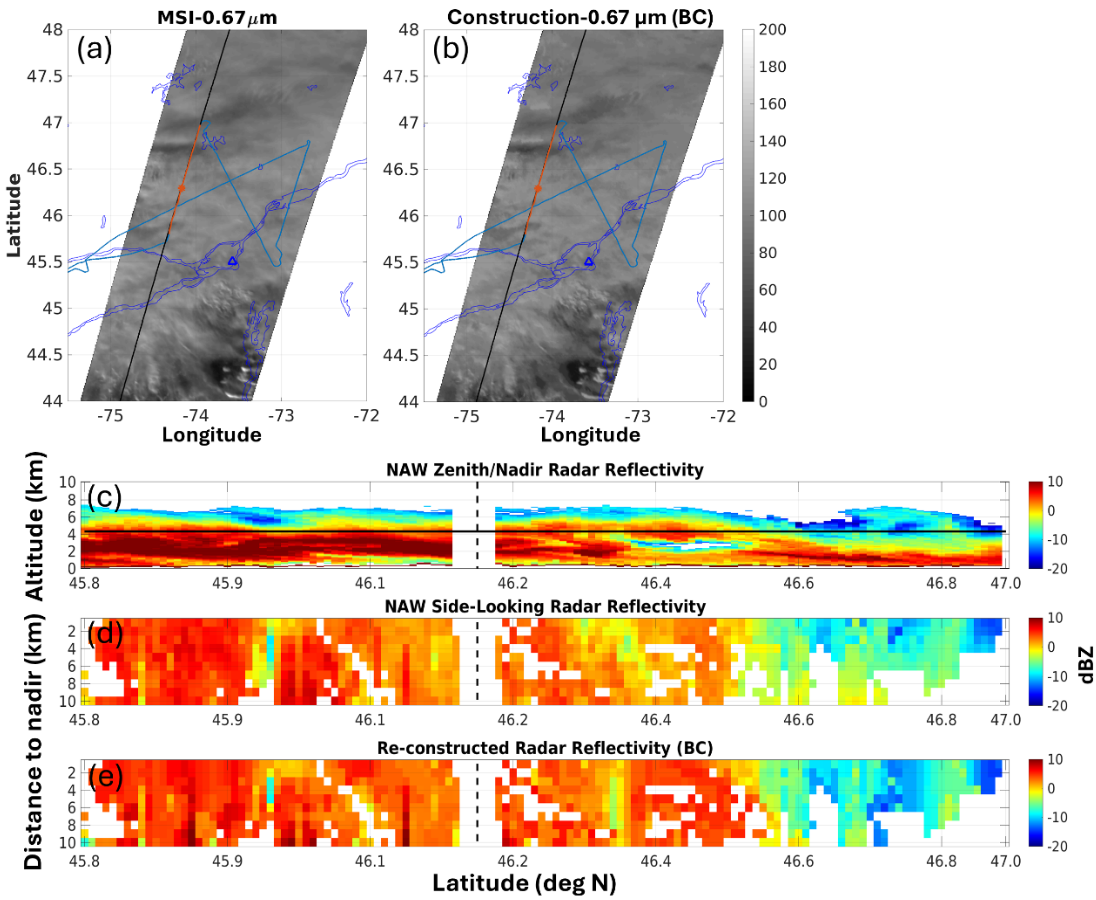

Figure 7: Scene construction validation using side-pointing NAW radar for ECALOT Flight 6 on 27 January 2025 (EarthCARE Frame 03794D). (a). MSI 0.67 µm radiances. Black line: EarthCARE nadir track, blue line: Convair-580 flight track, red line: underflight segment, red asterisk: colocation point between Convair-580 and EarthCARE, blue triangle: Montreal. (b). similar to (a), but reconstructed TOA radiances at 0.67 µm by ACMB-3D. (c). NAW zenith/nadir radar reflectivity. Black line: Conviar-580 flight altitude, dashed line: colocation location. (d). NAW side-looking radar reflectivity. (e). Re-constructed side pointing radar reflectivity using ACMB-3D baseline BC.

6.5. Surface and airborne radiative closure

EarthCARE performs operational radiative closure assessments using BBR observations at the TOA as a reference. This TOA-based approach provides important information for monitoring the overall consistency of the EarthCARE retrieval products. However, certain atmospheric conditions may require multiple viewing perspectives to adequately assess retrieval accuracy, as TOA-based closure alone may not be sensitive to deficiencies in the lower portions of cloud systems. This is particularly relevant for cases involving embedded mixed-phase layers, such as the nimbostratus cloud system observed during ECALOT

https://doi.org/10.5194/egusphere-2026-5347
Preprint. Discussion started: 9 September 2026

Flight 7 on 25 March 2025 (Figure 8). In this case, a supercooled liquid layer near cloud top is captured by the synergistic retrieval (ACM-CAP), and the corresponding TOA radiative closure shows good agreement between BBR observations (black line in Figure 10e & f) and simulated radiative fluxes (blue crosses in Figure 10e & f).

However, retrieval of LWC at lower altitudes is more challenging, as it approaches the sensitivity limits of the observing system. In particular, attenuation of the ATLID signal by the upper supercooled liquid layer can limit its ability to probe deeper cloud regions, reducing constraints on the vertical distribution of liquid water below. Consistent with this, in situ measurements at approximately 1.8 km altitude (black line in panel d & e of Figure 8) indicate the presence of mixed-phase conditions (positive LWC & IWC) over a substantial portion of the underflight segment, while the liquid component is largely absent in both EarthCARE's composite and synergy retrieval (blue & red lines in panel e). These mixed-phase layers influence radiative fluxes at lower levels, suggesting that surface- and aircraft-based radiative closure analyses provide complementary constraints for assessing EarthCARE retrieval performance. To address this, two complementary radiative closure approaches were implemented within ECALOT using observations from surface sites and aircraft nadir viewing.

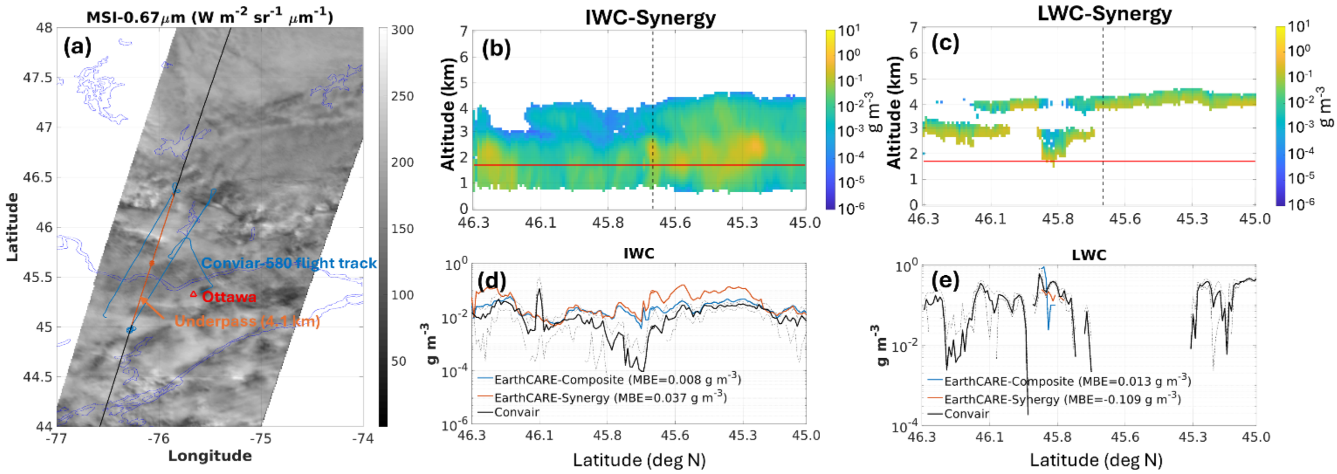

Figure 8. Underflight segment during ECALOT Flight 7 on 25 March 2025. The corresponding EarthCARE frame is 04681D. (a) MSI 0.67 µm spectral radiance. The black line indicates the EarthCARE ground track, the blue line the Convair-580 flight track, and the orange line the underflight segment. (b) Vertical cross-section along the underflight segment showing EarthCARE synergistic retrievals of IWC (ACM-CAP). The red line indicates the Convair-580 flight altitudes, and the dashed line marks the aircraft-satellite collocation point. (c) Same as (b), but for LWC. (d) IWC at the aircraft level. The black solid line shows the mean in situ measurements, with the dashed black lines indicating the standard deviation. The red and blue lines represent the synergistic (ACM-CAP, Baseline BC) and composite (ACM-COM, Baseline BC) retrievals, respectively. (e) Same as (d), but for LWC.

For the surface-based radiative closure, AERI instruments measuring spectral infrared radiance, together with broadband net radiometers, were deployed at all three surface sites. These instruments provide high-quality spectral and broadband radiation measurements, enabling both spectrally resolved and broadband radiative closure assessments using cloud profiles retrieved from EarthCARE. Although the surface sites are not located directly on the satellite nadir track, the scene construction algorithm can be used to reconstruct the three-dimensional cloud fields above the sites (see surface validation in Figure 1).

https://doi.org/10.5194/egusphere-2026-5347
Preprint. Discussion started: 9 September 2026

This approach allows evaluation of both EarthCARE-retrieved cloud properties (A-ICE, C-CLD, M-COP, ACM-COM, ACM-CAP) and the quality of the scene reconstruction (ACMB-3D) (Liu et al., 2026). In addition to the operational TOA-based radiative closure, the continuous surface observations provide the basis for routine surface-based closure analyses, offering complementary constraints on EarthCARE retrieval performance.

In addition to the constraints on mixed-phase cloud retrievals highlighted in Figure 8, surface radiative closure also provides useful constraints for stratocumulus cases. Figure 9 shows the surface radiative closure results for Flight 2 on 10 October 2024. Because of a data gap in the MSI observations, GOES-16 spectral radiances were used instead to support scene construction for the atmosphere column above the surface site (red dot in Figure 9a). Three cloud retrieval products, composite product version 11.4, composite product version 11.4 with an empirical correction, and synergy product version 11.4, were used as input to line-by-line radiative transfer simulations. The resulting simulated surface spectral radiances show varying degrees of agreement with the AERI observations, providing an independent assessment of the radiative consistency of the different retrievals. These comparisons therefore provide complementary constraints on EarthCARE liquid-cloud retrieval performance and support the broader calibration and validation effort. They also offer a complementary perspective to the in situ constraints on liquid-cloud vertical structure obtained from the aircraft porpoising measurements discussed in Section 6.3.

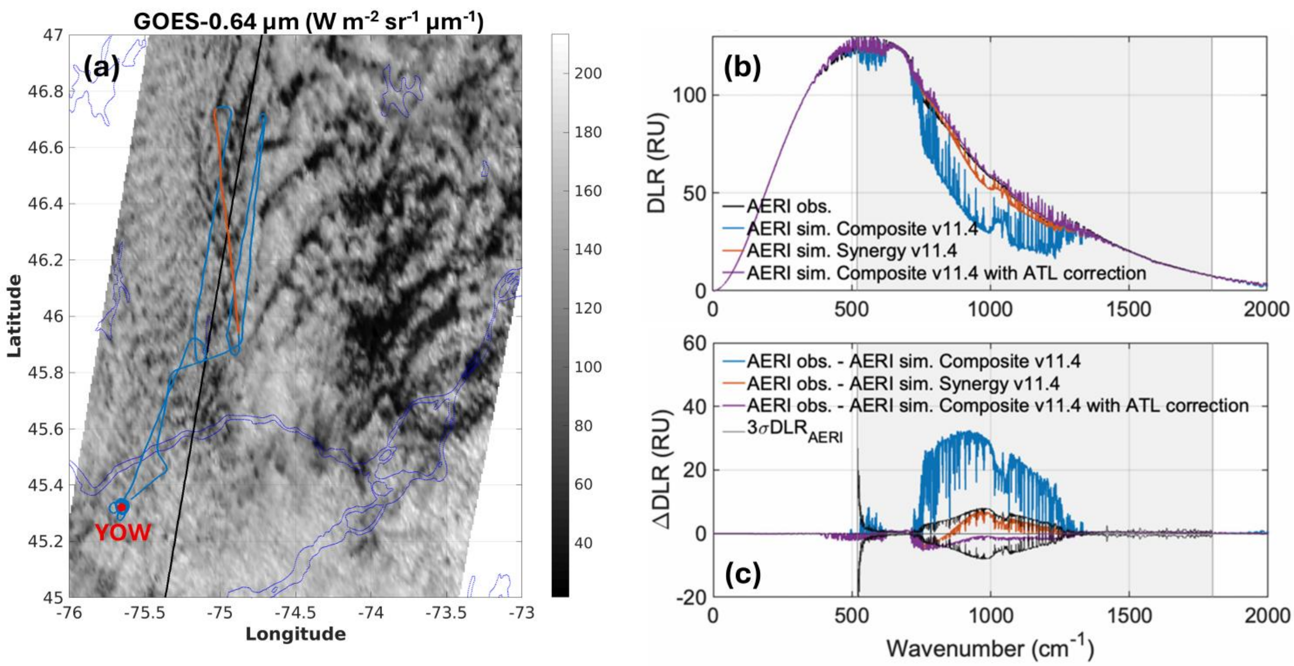

Figure 9: Spectral surface radiative closure using AERI observations and EarthCARE cloud retrievals for Oct. 10th, 2024 during Flight 2. (a). TOA radiance at 0.64 µm mapped onto the MSI swath using GOES-16 observations because of an MSI data gap during this frame. The red dot indicates the surface site at YOW. (b). Comparison between the AERI-observed spectrum (black) and simulated surface spectral radiance using EarthCARE cloud retrievals from the composite product version 11.40 (blue), the composite product version 11.40 with an empirical correction (purple), and the synergy product version 11.40 (orange). (c). Differences corresponding to the comparisons shown in (b), with black lines indicating the ±3σ range. DLR: downwelling longwave radiance; RU: radiance units (1 RU = 1 mW m^{-2} sr^{-1} cm).

https://doi.org/10.5194/egusphere-2026-5347
Preprint. Discussion started: 9 September 2026

For the aircraft-based radiative closure, during Flights 6 and 7, the FIRR-2 was installed aboard the Convair-580 aircraft (black FOV beam in Figure 1). Using EarthCARE-retrieved cloud properties, together with temperature and humidity profiles from auxiliary data, airborne radiative closure analyses can be performed along the satellite underflight track. This configuration provides an independent assessment of the consistency between retrieved atmospheric structure and observed radiative signatures at flight altitude. In particular, the airborne perspective offers additional insight into cases where mixed-phase cloud structures are not fully represented in the retrievals, such as the conditions observed during Flight 7 (Figure 8).

Radiative closure assessments performed at the surface (AERI and net radiometers) and at aircraft altitude (FIRR-2) provide complementary perspectives relative to the operational TOA radiative closure based on BBR aboard EarthCARE. In contrast to the broadband approach of BBR, these ECALOT measurements include high spectral resolution infrared (AERI), multi-spectral infrared (FIRR-2), and broadband (net radiometers) observations, offering additional constraints across different parts of the radiative spectrum. This multi-level and multi-spectral observational framework provides enhanced insight into the influence of internal cloud structure on radiative quantities and supports a more comprehensive evaluation of EarthCARE's retrieval performance.

Finally, radiative measurements from AERI, net radiometers, and FIRR-2 can be compared with broadband shortwave and longwave fluxes in ACM-RT. Broadband radiometers (e.g., net radiometers) allow direct comparison with simulated broadband quantities, whereas spectrally resolved instruments (AERI and FIRR-2) require spectral integration prior to broadband comparison (Liu et al., 2026). These comparisons support evaluation and validation of EarthCARE's radiative products.

6.6. Surface validation

In addition to the surface-based radiative closure described in Section 6.5, observations collected at the YOW surface site provide further opportunities to evaluate EarthCARE Level 1 and Level 2 products. Independent surface measurements offer complementary constraints on the atmospheric state and cloud properties, thereby contributing to the assessment of uncertainties across the EarthCARE data processing chain.

6.6.1. Auxiliary data validation

Atmospheric temperature and humidity profiles are critical inputs for the infrared radiative closure discussed in Section 6.5. These profiles are not retrieved directly by EarthCARE but are provided by the Integrated Forecasting System (IFS) (Bauer et al. 2015; ECMWF, 2024) of the European Centre for Medium-Range Weather Forecasts (ECMWF), with a horizontal resolution of approximately 9 km. Assessing the accuracy of these auxiliary profiles is important for quantifying their contribution to uncertainties in the radiative closure assessment mentioned in Section 6.5.

https://doi.org/10.5194/egusphere-2026-5347
Preprint. Discussion started: 9 September 2026

Several instruments deployed at the surface sites provide independent measurements relevant to this evaluation. Water vapor profiles are measured by the DA10 and MP3000 microwave radiometer, while temperature profiles are observed from the MP3000. These observations also enable comparisons with the auxiliary atmospheric state fields included in EarthCARE's Level 1 X-MET product, thereby supporting evaluation of the consistency and representativeness of the auxiliary data, which is used to define the atmospheric state in EarthCARE's radiative transfer calculations (e.g., ACM-RT processor).

6.6.2. Target classification and cloud base height

Surface instruments also provide information on precipitation occurrence, amount, and type, which can be used to assess EarthCARE target classification products during precipitation events (C-TC and AC-TC), as well as retrieved precipitation quantities (C-CLD, ACM-COM, ACM-CAP). Such comparisons are particularly useful for evaluating classification performance in mixed-phase and stratiform precipitation systems.

In addition, the cloud base height can be estimated from surface-based lidar observations. These measurements provide an independent reference for comparison with cloud base heights inferred from EarthCARE target classification and retrieval products, thereby offering further insight into the vertical representation of cloud structure.

6.7. Supercooled liquid layers and their radiative impact

ECALOT flights sampled a wide range of cloud regimes, including liquid, mixed-phase, and fully glaciated ice clouds. Several of these cloud types remain challenging to simulate in high-resolution NWP models, particularly under cold-season conditions. One example is the presence of supercooled liquid layers (SCLs) embedded within or at the top of nimbostratus systems, as observed during Flights 5 and 7. SCLs involve complex microphysical processes, including droplet activation, ice nucleation, depositional growth, and the Wegener-Bergeron-Findeisen process, whose representation in numerical models is sensitive to assumptions within cloud microphysics parameterizations (Korolev et al., 2017; Korolev and Milbrandt, 2022). Because aerosol-cloud interactions directly influence droplet activation and ice nucleation, the treatment of aerosols in the model can be critical to the formation and maintenance of SCLs (Cholette et al., 2026; Qu et al., 2026). In addition, the horizontal and vertical resolution of the numerical model can play an important role in determining whether thin or shallow SCLs are adequately represented (Qu et al., 2026). The horizontal resolution is critical for representing vertical water-vapour transport associated with fine-scale structures near cloud top, such as generating cells, whereas the vertical resolution is important for accurately resolving the cloud-top radiative heating and cooling-rate profiles.

An illustrative case from ECALOT Flight 7 is shown in Figure 10, in which a baseline simulation (HRDPS, Milbrandt et al., 2016) using Global Environmental Multi-scale Model (GEM, Côté et al., 1998; Girard et al., 2014; McTaggart-Cowan et al., 2019), with a horizontal grid spacing of 2.5 km and 84 vertical hybrid layers, does not reproduce the upper supercooled liquid layer (at 3-4 km altitude) observed in situ. Although this upper SCL is geometrically thin, with a depth of approximately 100 to 200 m, its radiative impact is substantial, as illustrated in panels (e) and (f) of Figure 10. The absence of this layer in the

https://doi.org/10.5194/egusphere-2026-5347
Preprint. Discussion started: 9 September 2026

simulation is associated with differences of approximately 200 W m^{-2} in shortwave and 10 to 20 W m^{-2} in longwave TOA upwelling fluxes. Such SCLs are frequently observed in mid- and high-latitude regions, indicating that inadequate representation of these layers can lead to substantial biases in simulated radiative fluxes and, consequently, in weather and climate model predictions.

To better characterize such vertically structured cloud systems, ECALOT provides in situ observations collected at multiple flight altitudes during different flight segments. These measurements offer vertically resolved information on liquid water content, ice water content, particle size distributions, and phase composition. Such observations are essential for (1) characterizing the thermodynamic and microphysical structure of clouds, (2) evaluating model representations of these structures, and (3) informing further development of cloud parameterization algorithms in NWP models. Improved representation of cloud properties is expected to lead to more accurate simulation of radiative quantities, thereby enhancing overall model performance.

https://doi.org/10.5194/egusphere-2026-5347
Preprint. Discussion started: 9 September 2026

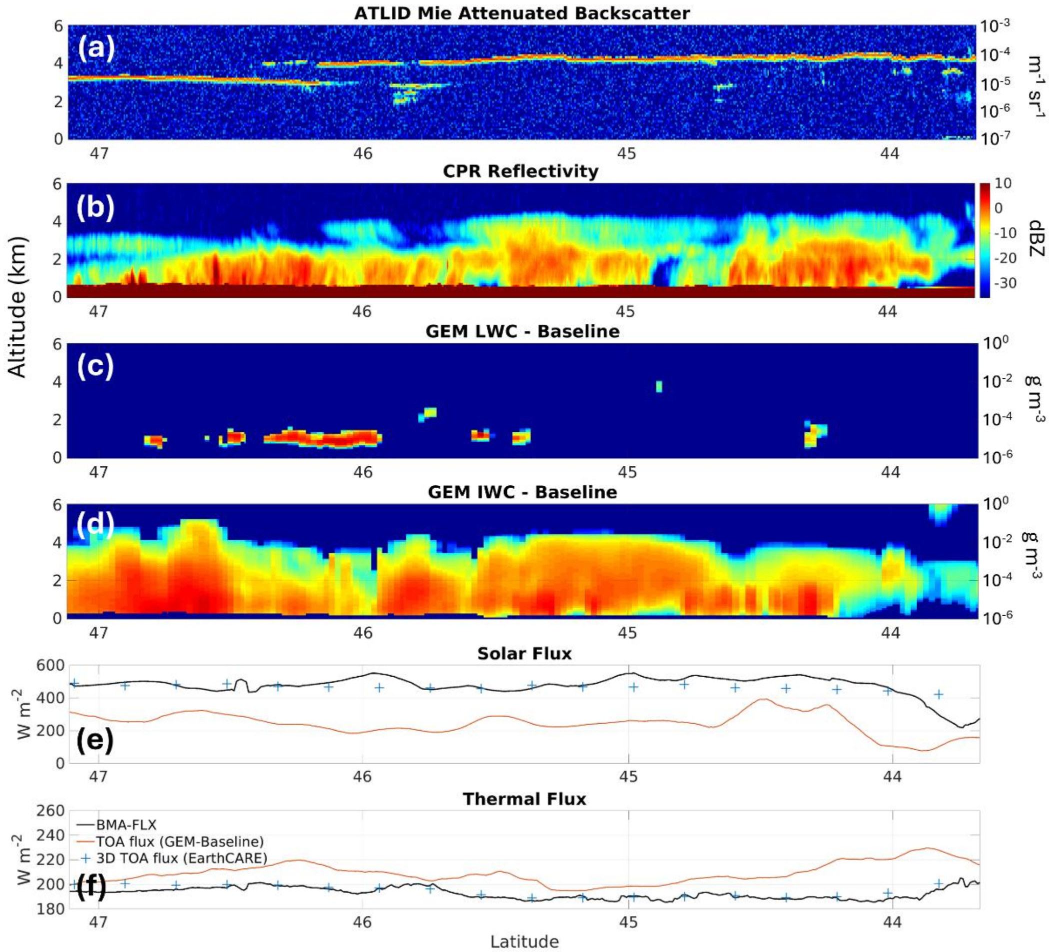

Figure 10: EarthCARE cross-section during ECALOT Flight 7 (04681D). (a). ATLID Mie attenuated backscatter, (b). CPR reflectivity and (c). GEM simulated liquid water content. (d). GEM simulated ice water content. (e). Shortwave TOA fluxes from BBR (black line), ACM-RT 3D Mont-Carlos radiative transfer simulation (blue crosses for the assessment domains) and GEM simulation (red line). (f). Similar to (e) but for longwave fluxes.

7. Conclusion and perspectives

The ECALOT campaign was conducted over the Ottawa-Montreal region and surrounding areas with coordinated airborne and surface observations. Dedicated research flights using the NRC Convair-580 aircraft combined along-track underpass segments with off-nadir sampling at multiple altitudes before and after satellite overpasses. These flights integrated vertically resolved remote sensing of clouds and aerosols, aircraft-level radiative measurements, and in situ observations of cloud, aerosol and atmospheric conditions within and adjacent to the satellite nadir cross-sections. Complementary surface sites were strategically positioned to provide continuous remote sensing and radiative measurements, thereby extending the temporal coverage and vertical context beyond the aircraft sampling window. Together, these observations provide a comprehensive

https://doi.org/10.5194/egusphere-2026-5347
Preprint. Discussion started: 9 September 2026

multi-platform reference dataset for independent assessment of EarthCARE products and for future studies of cloud, aerosol, precipitation, and radiation processes.

The products of EarthCARE span multiple stages of a complex processing chain, from Level 1 calibrated measurements to Level 2 processed observations, retrieved geophysical quantities, scene construction products, and radiative flux estimates. ECALOT was designed to address this multi-level framework through five complementary and interrelated pillars: (1) direct comparison of radar and lidar measurements between satellite and airborne platforms; (2) evaluation of cloud and aerosol retrievals using coordinated airborne in situ observations; (3) validation of cloud and precipitation properties through surface-based measurements; (4) assessment of scene construction products via off-nadir cloud characterization; and (5) radiative closure analyses linking retrieved atmospheric structure to observed radiative signatures at aircraft and surface levels.

This integrated approach represents a key strength of ECALOT, enabling EarthCARE products to be evaluated not only individually but also for their consistency across the EarthCARE processing chain over several seasons and varying terrain. Beyond calibration and validation objectives, the resulting multi-platform dataset also provides a high-quality benchmark for NWP model evaluation, supporting continued improvement of cloud parameterizations.

Although the campaign spanned three seasons, some cloud regimes remained underrepresented. In particular, liquid and mixed-phase stratocumulus cloud systems were sampled only to a limited extent, and additional cases are needed to better characterize their vertical structure and associated microphysical variability. Several challenges in EarthCARE cloud and precipitation retrievals also remain, including clouds containing relatively large ice particles at warmer temperatures between -5 and -2 °C, retrievals within and below the melting layer, rain properties, mixed-phase conditions across different cloud regimes, and wildfire smoke. Future coordinated aircraft campaigns will target these conditions to further evaluate EarthCARE products and support continued improvements in retrieval performance.

All ECALOT observations were systematically archived and subjected to standardized QC and QA procedures to ensure data quality and consistency. Preliminary checks conducted during operations were complemented by post-campaign processing and verification, resulting in a consolidated dataset suitable for quantitative comparison with satellite measurements. Datasets were converted to GEOMS format and submitted to the ESA Validation Data Centre (EVDC) to facilitate cal/val analyses.

Together, ECALOT observations establish a foundation for systematic EarthCARE cal/val across a broader range of cloud regimes, while the identified gaps provide a clear basis for targeting future coordinated campaigns.

Appendix A: Selected examples of EarthCARE cal/val campaigns and contributing observational networks

Table A**1** summarizes the full names of the EarthCARE cal/val campaigns, contributing observational networks, and research infrastructures referred to in Sect. 1. The entries represent a subset of the broader international EarthCARE cal/val effort and include airborne campaigns, ground-based validation networks, research infrastructures, and radiative closure activities.

https://doi.org/10.5194/egusphere-2026-5347
Preprint. Discussion started: 9 September 2026

Table A1: Full names and general characteristics of EarthCARE cal/val campaigns, observational networks, and research infrastructures referred to in this study.

Acronym	Full campaign name	Type	Main region / environment
PERCUSION	Persistent EarthCARE Underflight Studies of the ITCZ and Organized Convection	Airborne campaign	Tropical Atlantic
CELLO	Cloud and EarthCARE caL/vaL Observations		Tropical Atlantic
PACE-PAX	Plankton, Aerosol, Cloud, ocean Ecosystem Postlaunch Airborne eXperiment		Southern and Central California / nearby coastal region
ARCSIX	Arctic Radiation-Cloud-Aerosol-Surface Interaction EXperiment		Arctic/Greenland
MORECALVAL	MObile Radar-Lidar-Radiometer EarthCARE CAL/VAL		Europe/mid-latitudes
VERIFY	VERIFY campaign		United Kingdom/mid-latitudes
PONEX	Polar Night Experiment		Canadian Arctic
COMPEX-EC	Clouds over cOMPlEX environment - EarthCARE		Arctic/northern Scandinavia
NightBLUE	Nighttime Bermuda Lidar Underflights of EarthCARE		Bermuda/North Atlantic
NAWDIC-DICHOTOMI	North Atlantic Waveguide, Dry Intrusion, and Downstream Impact Campaign – Dry Intrusion and Cloud Head winds On Top Of Marine Interfaces		North Atlantic/western Europe
HALO-South	The interplay of Clouds, Aerosols and Radiation above the Southern Ocean		Southern Ocean/New Zealand
PollyNET	Portable Lidar System Network	Ground-based lidar network	Ground-based lidar network, including ACTRIS and associated sites
ACTRIS	Aerosol, Clouds and Trace Gases Research Infrastructure	Research infrastructure	Ground-based European research infrastructure/distributed sites
RACE-ECV	Radiation Closure Experiments for EarthCARE Validation	Ground-based campaign	Surface-based radiative closure; Thessaloniki, Greece

Code, data, or code and data availability

ECALOT data are available through the ESA Validation Data Centre (EVDC) data portal (https://evdc.esa.int/search/) (ESA, n.d.). Users must register and log in to access and download the datasets, which can be searched and filtered by location, data source type, scientific discipline, campaign, and other metadata. The portal also provides quick-look visualizations for data inspection. EarthCARE satellite products used in this study are available through the EarthCARE Multi-Mission Algorithm and Analysis Platform (MAAP) (https://portal.maap.eo.esa.int/earthcare/) (ESA, 2025). The GEM code (version 5.3.0-a10) is available from https://github.com/ECCC-ASTD-MRD/gem/releases/tag/5.3.0-a10 (ECCC, 2024).

https://doi.org/10.5194/egusphere-2026-5347
Preprint. Discussion started: 9 September 2026

Author contributions

ZQ, CN, PB, AK, HWB, KR, ZM, LN, YH, JNSC, EB, JG, JMT, and KAW contributed to the conceptualization and design of ECALOT. CN, PB, AK, KR, KB, IH, NB, LN, RP, JPB, YB, MiW, and MeW contributed to airborne observations, instrument operation, and airborne data processing. SH, RR, RC, ZM, EB, LL, YH, BRB, and JMT contributed to surface observations and ground-based data processing. MK, RC, ZM, BRB, CN, KR, and LL contributed to data format conversion and archiving. MC, JAM, and ZQ contributed to modelling support. MPS provided satellite orbit calculations. JvB, RK, ZQ, DM, CN, LN, NB, YH, JMT, and KAW contributed to project administration or institutional coordination. ZQ, PB, CN, KR, LL, ZM, HWB, YH, BRB, RP, JNSC, BPT, RJH, and SLM performed the analysis and interpretation presented in this paper. ZQ led preparation of the original manuscript draft, with contributions from CN, PB, AK, KR, LL, ZM, MK, RP, BRB, RJH, and BPT. All authors contributed to the discussion of the results, manuscript review and editing, and approved the final version.

Acknowledgements

The ECALOT team gratefully acknowledges the NRC flight crew, Anthony Brown, Reagh Sherwood and Bryan Carrothers, for their precision and flexibility in executing coordinated underflights. We also thank the NRC technical support team, including Éric Roux and Daniel MacDonald, for their essential assistance with aircraft integration and instrument operations. We acknowledge the support from ESA colleagues Stephanie Rusli and Vasileios Tzallas for their guidance and coordination during campaign planning and implementation. Finally, we appreciate the assistance of Ian Boyd and Ann Mari Fjæraa from EVDC in facilitating data handling and archiving.

Financial support

The ECALOT campaign was co-funded by ESA under contract no. 4000145188/24/NL/FFi. Surface observations were supported by the ECCC Grants and Contributions Program under reference no. GCXE25S072. ECCC also provided in-kind personnel contributions, while NRC provided in-kind personnel and aircraft operation support via its Environmental Science focus area in the Aerospace Research Center (project #ES-009). Additional in-kind contributions were provided by McGill University, Université du Québec à Montréal, and the University of Toronto through personnel time, instrumentation, data processing, and scientific support.

References

Amiridis, V., Marinou, E., Hostetler, C., Koopman, R., Cecil, D., Moisseev, D., Tackett, J., Groß, S., Baars, H., Redemann, J., Marenco, F., Baldini, L., Tanelli, S., Fielding, M., Janiskova, M., Tanaka, T., O'Connor, E., Fjaeraa, A. M., Paschou, P., Voudouri, K. A., Ferrare, R., Burton, S., Schuster, G., Kato, S., Winker, D., Shook, M., Bley, S., Haarig, M., Floutsi, A. A., Wandinger, U., Trapon, D., Pfitzenmaier, L., Papagiannopoulos, N., Mona, L., Posselt, D., Mason, S., Rennie, M., Benedetti, A., Hogan, R., Sogacheva, L., Balis, D., Michailidis, K., van Zadelhoff, G.-J., Nowottnick, E., Yorks, J., Mroz, K., Donovan, D., L'Ecuyer, T., Okamoto, H., Sato, K., Henderson, D., Nishikawa, T., Barker, H., Cole, J., Qu, Z., Clerbaux, N., Nakajima, T., Chase, R., Wolff, D., Landulfo, E., Kirstetter, P.-E., Mather, J., Ohigashi, T., Ryder, C., Tzallas, V., Tsikoudi, I., Tsekeri, A., Tsichla, M., Koutsoupi, I., Kubota, T., Siomos, N., Takahashi, N., Horie, H., Suzuki, K., Mace, J., McLean, W., Borderies, M., Mangla, R., Escribano, J., Moradi, I., Zhang, J., Juli, R., Ikuta, Y., Marbach, T., Bojkov, B., Accadia, C., Fougnie, B., Spezzi, L., Bozzo, A., Chimot, J., Jafariserajehlou, S., Flament, T., Mattioli, V., Strandgren, J., Barlakas, V., and Kollias, P.: Best Practice Protocol for the validation of Aerosol, Cloud, and Precipitation Profiles (ACPPV) (Version 2), Zenodo, https://doi.org/10.5281/zenodo.15025627, 2025.

Aoki, S., Kubota, T., and Turk, F. J.: Exploring vertical motions in convective and stratiform precipitation using spaceborne radar observations: insights from EarthCARE and GPM coincidence dataset, Atmos. Meas. Tech., 19, 79–100, https://doi.org/10.5194/amt-19-79-2026, 2026.

Baibakov, K., Wolde, M., Nguyen, C., Korolev, A& Wechsler, P.: Performance of a compact elastic 355 nm airborne lidar in tropical and mid-latitude clouds. Lidar Technologies, Techniques, and Measurements for Atmospheric Remote Sensing XI (Vol. 10006, pp. 45-55). SPIE, DOI:10.1117/12.2242112, 2016.

Barker, H. W., Cole, J. N. S., and Shephard, M.: Estimation of Errors associated with the EarthCARE 3D Scene Construction Algorithm. Q. J. R. Meteorol. Soc., 140, 2260–2271, DOI:10.1002/qj.2294, 2014.

Barker, H. W., Cole, J. N. S., Villefranque, N., Qu, Z., Velázquez Blázquez, A., Domenech, C., Mason, S. L., and Hogan, R. J.: Radiative closure assessment of retrieved cloud and aerosol properties for the EarthCARE mission: the ACMB-DF product, Atmos. Meas. Tech., 18, 3095–3107, https://doi.org/10.5194/amt-18-3095-2025, 2025.

Barker, H. W., Gabriel, P. M., Qu, Z., and Kato, S.: Representativity of cloud-profiling radar observations for data assimilation in numerical weather prediction, Q. J. R. Meteorol. Soc., 147, 103–123, https://doi.org/10.1002/qj.3996, 2021.

Barker, H. W., Jerg, M. P., Wehr, T., Kato, S., Donovan, D., and Hogan, R.: A 3D Cloud Construction Algorithm for the EarthCARE satellite mission. Q, J. R. Meteorol. Soc., 137, 1042–1058 DOI:10.1002/qj.824, 2011.

Barker, H. W., Kato, S., and Wehr, T.: Computation of Solar Radiative Fluxes by 1D and 3D Methods using Cloudy Atmospheres Inferred from A-train Satellite Data. Surveys in Geophys. 33, 657-676, 2012.

Barker, H. W., Korolev, A. V., Hudak, D. R., Strapp, J. W., Strawbridge, K. B., and Wolde, M.: A comparison between CloudSat and aircraft data for a multilayer, mixed-phase cloud system during the Canadian CloudSat-CALIPSO Validation Project, J. Geophys. Res., 113, D00A16, https://doi.org/10.1029/2008JD009971, 2008.

https://doi.org/10.5194/egusphere-2026-5347
Preprint. Discussion started: 9 September 2026

Barrett, A. I., Hogan, R. J., and Forbes, R. M.: Why are mixed-phase altocumulus clouds poorly predicted by large-scale models? Part 2. Vertical resolution sensitivity and parameterization, J. Geophys. ResBarker, H. W., Stephens, G. L., Partain, P. T., Bergman, J. W., Bonnel, B., Campana, K., et al.: Assessing 1-D atmospheric solar radiative transfer models: Interpretation and handling of unresolved clouds, J. Climate, 16, 2676–2699, https://doi.org/10.1175/1520-0442(2003)016<2676:ADASRT>2.0.CO;2, 2003.

Baars, H., Haarig, M., König, L., Floutsi, A. A., Basharova, E., Hofer, J., Gebauer, H., Engelmann, R., Althausen, D., Skupin, A., Gast, B., Fritzsch, F., Ohneiser, K., Jimenez, C., Gaudek, T., Radenz, M., Buholdt, H., Heese, B., Klamt, A., Seifert, P., Donovan, D. P., van Zadelhoff, G.-J., Abdullaev, S. F., Khalifaeva, S. K., Nozirov, D. F., and Wandinger, U.: Validation of EarthCARE/ATLID aerosol profiling products with ground-based PollyNET lidars – case studies, Atmos. Meas. Tech., 19, 3831–3864, https://doi.org/10.5194/amt-19-3831-2026, 2026.

Bauer, P., Thorpe, A., and Brunet, G.: The quiet revolution of numerical weather prediction, *Nature*, 525, 47–55, https://doi.org/10.1038/nature14956, 2015.

Boudala, F. S., Lachapelle, M., Isaac, G. A., Milbrandt, J. A., Michelson, D., Reed, R., and Holden, S.: Observations of the microphysics and type of wintertime mixed-phase precipitation, and instrument comparisons at Sorel, Quebec, Canada, Remote Sens., 17, 945, https://doi.org/10.3390/rs17060945, 2025.

Cetinić, I., Knobelspiesse, K., Cairns, B., and Piñol Solé, M.: PACE-PAX validation campaign – validating PACE and supporting EarthCARE, EGU General Assembly 2024, Vienna, Austria, EGU24-20116, https://doi.org/10.5194/egusphere-egu24-20116, 2024.

Cholette, M., Thériault, J. M., Milbrandt, J. A., and Morrison, H.: Impacts of predicting the liquid fraction of mixed-phase particles on the simulation of an extreme freezing rain event: The 1998 North American Ice Storm, Mon. Weather Rev., 148, 3799–3823, https://doi.org/10.1175/MWR-D-20-0026.1, 2020.

Cholette, M., Jouan, C., Morrison, H., Milbrandt, J. A., Qu, Z., Dedekind, Z., Korolev, A., and Mariani, Z.: Introduction of prognostic aerosols in the P3 microphysics scheme: Simulation of layered Arctic mixed-phase clouds, EGUsphere [preprint], https://doi.org/10.5194/egusphere-2026-4229, 2026.

Cole, J. N. S., Barker, H. W., Qu, Z., Villefranque, N., and Shephard, M. W.: Broadband radiative quantities for the EarthCARE mission: the ACM-COM and ACM-RT products, Atmos. Meas. Tech., 16, 4271–4288, https://doi.org/10.5194/amt-16-4271-2023, 2023.

Cober, S. G., Isaac, G. A., Korolev, A. V., and Strapp, J. W.: Assessing cloud-phase conditions, J. Appl. Meteorol., 40, 1967–1983, https://doi.org/10.1175/1520-0450(2001)040<1967:ACPC>2.0.CO;2, 2001.

https://doi.org/10.5194/egusphere-2026-5347
Preprint. Discussion started: 9 September 2026

Côté, J., Gravel, S., Méthot, A., Patoine, A., Roch, M., and Staniforth, A.: The operational CMC–MRD global environmental multiscale (GEM) model. Part I: Design considerations and formulation, Mon. Weather Rev., 126, 1373–1395, 1998.

Delanoë, J.: MORECALVAL: MObile Radar-Lidar-Radiometer EarthCare CAL/VAL project, ESA–JAXA EarthCARE Validation Workshop, presentation, 2023.

De Mazière, M., Thompson, A. M., Kurylo, M. J., Wild, J. D., Bernhard, G., Blumenstock, T., Braathen, G. O., Hannigan, J. W., Lambert, J.-C., Leblanc, T., McGee, T. J., Nedoluha, G., Petropavlovskikh, I., Seckmeyer, G., Simon, P. C., Steinbrecht, W., and Strahan, S. E.: The Network for the Detection of Atmospheric Composition Change (NDACC): history, status and perspectives, Atmos. Chem. Phys., 18, 4935–4964, https://doi.org/10.5194/acp-18-4935-2018, 2018.

Docter, N., Hünerbein, A., Donovan, D. P., Preusker, R., Fischer, J., Meirink, J. F., Stammes, P., and Eisinger, M.: Assessment of the spectral misalignment effect (SMILE) on EarthCARE's Multi-Spectral Imager aerosol and cloud property retrievals, Atmos. Meas. Tech., 17, 2507–2519, https://doi.org/10.5194/amt-17-2507-2024, 2024.

Donovan, D. P., van Zadelhoff, G.-J., and Wang, P.: The EarthCARE lidar cloud and aerosol profile processor (A-PRO): the A-AER, A-EBD, A-TC, and A-ICE products, Atmos. Meas. Tech., 17, 5301–5340, https://doi.org/10.5194/amt-17-5301-2024, 2024.

Donovan, D. P., Whiteway, J. and Carswell, A. I.: Correction for nonlinear photon-counting effects in lidar systems, Appl. Opt., 32, 6742–6753, https://doi.org/10.1364/AO.32.006742, 1993.

Environment and Climate Change Canada (ECCC): The Global Environmental Multiscale Model (GEM) (version 5.3.0-a10), GitHub [code], https://github.com/ECCC-ASTD-MRD/gem/releases/tag/5.3.0-a10 (last access 2 September 2026), 2024.

Eisinger, M., Marnas, F., Wallace, K., Kubota, T., Tomiyama, N., Ohno, Y., Tanaka, T., Tomita, E., Wehr, T., and Bernaerts, D.: The EarthCARE mission: science data processing chain overview, Atmos. Meas. Tech., 17, 839–862, https://doi.org/10.5194/amt-17-839-2024, 2024.

European Centre for Medium-Range Weather Forecasts (ECMWF): IFS Documentation, European Centre for Medium-Range Weather Forecasts, Reading, UK, available at: https://www.ecmwf.int/en/publications/ifs-documentation, 2024. (last access: 25 February 2026).

ESA: EarthCARE Multi-Mission Algorithm and Analysis Platform (MAAP), ESA [data portal], https://portal.maap.eo.esa.int/earthcare/ (last access 2 September 2026), 2025.

European Space Agency (ESA): EarthCARE Scientific Validation Implementation Plan (EC-PL-ESA-SYS-1049), Version 2.0, 6 September 2024, available at: https://www.eorc.jaxa.jp/EARTHCARE/document/2024-09-06%20EC-PL-ESA-SYS-1049%20EC%20Validation%20Plan%20-2.0%20_RKTKKW.pdf. (last access: 17 February 2026), 2024.

ESA: ESA Validation Data Centre (EVDC), ESA [data portal], https://evdc.esa.int/ (last access 2 September 2026), n.d.

https://doi.org/10.5194/egusphere-2026-5347
Preprint. Discussion started: 9 September 2026

Fan, J., Ghan, S., Ovchinnikov, M., Liu, X., Rasch, P. J., and Korolev, A.: Representation of Arctic mixed-phase clouds and the Wegener–Bergeron–Findeisen process in climate models: Perspectives from a cloud-resolving study, J. Geophys. Res. Atmos., 116, D00T06, https://doi.org/10.1029/2010JD015375, 2011.

Feenstra, T. N., van de Berg, W. J., van Zadelhoff, G.-J., Donovan, D. P., van Dalum, C. T., and van den Broeke, M. R.: Exploring new EarthCARE observations for evaluating Greenland clouds in RACMO2.4, EGUsphere [preprint], https://doi.org/10.5194/egusphere-2025-5623, 2025.

Field, P. R., Heymsfield, A. J., and Bansemer, A.: Shattering and particle interarrival times measured by optical array probes in ice clouds, J. Atmos. Oceanic Technol., 23, 1357–1371, https://doi.org/10.1175/JTECH1922.1, 2006.

Fielding, M. and Janiskova, M.: Preparations for operational use of EarthCARE data, ECMWF, https://doi.org/10.21957/335541d54a, 2023. (accessed 17 February 2026)

François, E., Delanoë, J., Mathon, T., and Baudoux, A.: Comparison between EarthCARE and airborne measurements and products during the MORECALVAL field campaign (L2 products), EarthCARE Science and Validation Workshop 2025, Tokyo, Japan, 1–5 December 2025, presentation, https://www.eorc.jaxa.jp/EARTHCARE/event/ws2025/program-data/H420_francois.pdf (last access: 2 September 2026), 2025.

François, E., Delanoë, J., Rivière, G., Baudoux, A., Jourdan, O., and the DICHOTOMI Team: Comparisons between EarthCARE and ATR42 during the NAWDIC-DICHOTOMI field campaign (L2a and L2b products), EarthCARE Science and Validation Workshop 2026, Oxford, UK, 8–12 June 2026, presentation, https://airdrive.eventsair.com/eventsairwesteuprod/production-nikal-public/da3b974bf8414e5fb7da9b6a43d9f8f3 (last access: 2 September 2026), 2026.

Furtado, K., Field, P. R., Boutle, I. A., Morcrette, C. J., and Wilkinson, J. M.: A physically based subgrid parameterization for the production and maintenance of mixed-phase clouds in a general circulation model, J. Atmos. Sci., 73, 279–291, https://doi.org/10.1175/JAS-D-15-0021.1, 2016.

Galfione, A., Battaglia, A., Puigdomènech Treserras, B., and Kollias, P.: First insights into deep convection by the Doppler velocity measurements of the EarthCARE Cloud Profiling Radar, Atmos. Meas. Tech., 18, 6747–6763, https://doi.org/10.5194/amt-18-6747-2025, 2025.

Girard, C., Desgagné, M., McTaggart-Cowan, R., Côté, J., Charron, M., Gravel, S., Lee, V., Patoine, A., Qaddouri, A., Roch, M., Spacek, L., Tanguay, M., Vaillancourt, P. A., and Zadra, A.: Staggered vertical discretization of the Canadian environmental multiscale (GEM) model using a coordinate of the log-hydrostatic-pressure type, Mon. Weather Rev., 142, 1183–1196, 2014.

https://doi.org/10.5194/egusphere-2026-5347
Preprint. Discussion started: 9 September 2026

Groß, S., Ewald, F., Stevens, B., Wirth, M., Dekoutsidis, G., Ehrlich, A., Kouklaki, D., Krüger, K., Rosenburg, S., Volkmer, L., von Bismarck, J., Hirsch, L., Luebke, A. E., Marinou, E., Mayer, B., Pinol Sole, M., Wendisch, M., Windmiller, J., Amiridis, V., Koopman, R., Kubota, T., and Rapp, M.: Persistent EarthCARE underflight studies of the ITCZ and organized convection (PERCUSION): contribution to EarthCARE validation, Atmos. Meas. Tech., 19, 3933–3959, https://doi.org/10.5194/amt-19-3933-2026, 2026.

Haarig, M., Hünerbein, A., Wandinger, U., Docter, N., Bley, S., Donovan, D., and van Zadelhoff, G.-J.: Cloud top heights and aerosol columnar properties from combined EarthCARE lidar and imager observations: the AM-CTH and AM-ACD products, Atmos. Meas. Tech., 16, 5953–5975, https://doi.org/10.5194/amt-16-5953-2023, 2023.

Hemminga, D., Wang, P., van Zadelhoff, G.-J., Donovan, D., von Bismarck, J., Hair, J., Nehrir, A., Ferrare, R., Hostetler, C., Shingler, T., Fenn, M., and Scarino, A. J.: Validation of ATLID products based on dedicated underflights from NASA aircraft campaigns ARCSIX, PACE-PAX and NightBLUE, EarthCARE Science and Validation Workshop 2025, Tokyo, Japan, 1–5 December 2025, presentation, https://www.eorc.jaxa.jp/EARTHCARE/event/ws2025/program-data/H422_Hemminga_updated.pdf (last access: 2 September 2026), 2025.

Hogan, R. J., Fielding, M. D., Barker, H. W., Villefranque, N., and Schäfer, S. A. K.: Entrapment: An important mechanism to explain the shortwave 3-D radiative effect of clouds, J. Atmos. Sci., 76, 2123–2141, https://doi.org/10.1175/JAS-D-18-0366.1, 2019.

Hogan, R. J., Puigdomenech Treserras, B., Mason, S. L., Korolev, A., Qu, Z., Mroz, K., Donovan, D. P., Kollias, P., and Fielding, M. D.: Evaluation of EarthCARE retrievals of ice microphysics and vertical wind using in-situ aircraft observations, EGUsphere [preprint], https://doi.org/10.5194/egusphere-2026-5054, 2026.

Huang, Y., Wu, W., McFarquhar, G. M., Wang, X., Morrison, H., Ryzhkov, A., Hu, Y., Wolde, M., Nguyen, C., Schwarzenboeck, A., et al.: Microphysical processes producing high ice water contents (HIWCs) in tropical convective clouds during the HAIC-HIWC field campaign: evaluation of simulations using bulk microphysical schemes, Atmospheric Chemistry and Physics, 21, 6919–6944, https://doi.org/10.5194/acp-21-6919-2021, 2021.

Huang, Y., Wu, W., McFarquhar, G. M., Xue, M., Morrison, H., Milbrandt,Korolev, A. V., Hu, Y., Qu, Z., Wolde, M., Nguyen, C., Schwarzenboeck, A., and Heckman, I.: Microphysical processes producing high ice water contents (HIWCs) in tropical convective clouds during the HAIC-HIWC field campaign: dominant role of secondary ice production, Atmos. Chem. Phys., 22, 2365–2384, https://doi.org/10.5194/acp-22-2365-2022, 2022.

Hünerbein, A., Bley, S., Deneke, H., Meirink, J. F., van Zadelhoff, G.-J., and Walther, A.: Cloud optical and physical properties retrieval from EarthCARE multi-spectral imager: the M-COP products, Atmos. Meas. Tech., 17, 261–276, https://doi.org/10.5194/amt-17-261-2024, 2024.

https://doi.org/10.5194/egusphere-2026-5347
Preprint. Discussion started: 9 September 2026

Illingworth, A., Barker, H., Beljaars, A., Ceccaldi, M., Chepfer, H., Delanoe, J., Domenech, C., Donovan, D., Fukuda, S., Hirakata, M., Hogan, R., Huenerbein, A., Kollias, P., Kubota, T., Nakajima, T., Nakajima, T., Nishizawa, T., Ohno, Y., and Okamoto, H.: The EarthCARE satellite: The next step forward in global measurements of clouds, aerosols, precipitation and radiation, Bull. Am. Meteorol. Soc., 96, 1311–1332, https://doi.org/10.1175/BAMS-D-12-00227.1, 2015.

Irbah, A., Delanoë, J., van Zadelhoff, G.-J., Donovan, D. P., Kollias, P., Puigdomènech Treserras, B., Mason, S., Hogan, R. J., and Tatarevic, A.: The classification of atmospheric hydrometeors and aerosols from the EarthCARE radar and lidar: the A-TC, C-TC and AC-TC products, Atmos. Meas. Tech., 16, 2795–2820, https://doi.org/10.5194/amt-16-2795-2023, 2023.

Isaac, G. A., Ayers, J., Bailey, M., Bissonnette, L., Bernstein, B., Cober, S., Driedger, N., Evans, W., Fabry, F., Glazer, A., Gultepe, I., Hallett, J., Hudak, D., Korolev, A., and Marcotte, D.: First results from the Alliance Icing Research Study II, 45th AIAA Aerospace Sciences Meeting and Exhibit, AIAA Paper 2005-252, https://doi.org/10.2514/6.2005-252, 2005.

Kazadzis, S. and the RACE ECV Thessaloniki Campaign Team: Assessing aerosol impacts on EarthCARE radiative closure using spectral radiation observations, EGU General Assembly 2026, EGU26-1791, https://doi.org/10.5194/egusphere-egu26-1791, 2026.

Khaykin, S., Sicard, M., Leblanc, T., Sakai, T., Balugin, N., Berthet, G., Chevrier, S., Chouza, F., Feofilov, A., Gantois, D., Godin-Beekmann, S., Haddouche, A., Jin, Y., Morino, I., Kadygrov, N., Lecas, T., Liley, B., Querel, R., Taha, G., and Yushkov, V.: Global transport of stratospheric aerosol produced by Ruang eruption from EarthCARE ATLID, limb-viewing satellites and ground-based lidar observations, Atmos. Chem. Phys., 26, 607–622, https://doi.org/10.5194/acp-26-607-2026, 2026.

Knuteson, R. O., Revercomb, H. E., Best, F. A., Ciganovich, N. C., Dedecker, R. G., Dirkx, T. P., Ellington, S. C., Feltz, W. F., Garcia, R. K., Howell, H. B., Smith, W. L., Short, J. F., and Tobin, D. C.: Atmospheric Emitted Radiance Interferometer. Part II: Instrument performance, J. Atmos. Oceanic Technol., 21, 1777–1789, https://doi.org/10.1175/JTECH-1663.1, 2004.

Kollias, P., Puigdomènech Treserras, B., Battaglia, A., Borque, P. C., and Tatarevic, A.: Processing reflectivity and Doppler velocity from EarthCARE's cloud-profiling radar: the C-FMR, C-CD and C-APC products, Atmos. Meas. Tech., 16, 1901–1914, https://doi.org/10.5194/amt-16-1901-2023, 2023.

Kollias, P., McFarquhar, G. M., Bruning, E., DeMott, P. J., Kumjian, M. R., Lawson, P., Lebo, Z., Logan, T., Lombardo, K., Oue, M., Roberts, G., Shaw, R. A., van den Heever, S. C., Wolde, M., et al.: Experiment of Sea Breeze Convection, Aerosols, Precipitation, and Environment (ESCAPE), B. Am. Meteorol. Soc., 106, E310–E332, https://doi.org/10.1175/BAMS-D-23-0014.1, 2025.

Korolev, A. and Field, P. R.: Assessment of the performance of the inter-arrival time algorithm to identify ice shattering artifacts in cloud particle probe measurements, Atmos. Meas. Tech., 8, 761–777, https://doi.org/10.5194/amt-8-761-2015, 2015.

https://doi.org/10.5194/egusphere-2026-5347
Preprint. Discussion started: 9 September 2026

Korolev, A. and Isaac, G. A.: Shattering during sampling by OAPs and HVPS. Part I: Snow particles, J. Atmos. Oceanic Technol., 22, 528–542, https://doi.org/10.1175/JTECH1720.1, 2005.

Korolev, A. and Leisner, T.: Review of experimental studies of secondary ice production, Atmos. Chem. Phys., 20, 11767–11797, https://doi.org/10.5194/acp-20-11767-2020, 2020.

Korolev, A. and Milbrandt, J. A.: How are mixed-phase clouds mixed? Geophys. Res. Lett., 49, e2022GL099578, https://doi.org/10.1029/2022GL099578, 2022.

Korolev, A., McFarquhar, G., Field, P. R., Franklin, C., Lawson, P., Wang, Z., Williams, E., Abel, S. J., Axisa, D., Borrmann, S., Crosier, J., Fugal, J., Krämer, M., Lohmann, U., Schlenczek, O., Schnaiter, M., and Wendisch, M.: Mixed-phase clouds: Progress and challenges, Meteorol. Monogr., 58, 5.1–5.50, https://doi.org/10.1175/AMSMONOGRAPHS-D-17-0001.1, 2017.

Korolev, A. V. and Strapp, J. W.: Accuracy of measurements of cloud ice water content by the Nevzorov probe, Preprints, AIAA 40th Aerospace Science Meeting and Exhibit, AIAA 2002-0679, Reno, NV, American Institute of Aeronautics and Astronautics, 1–8, 2002.

Korolev, A. V., Strapp, J. W., and Isaac, G. A.: Evaluation of the accuracy of PMS optical array probes, J. Atmos. Oceanic Technol., 15, 708–720, https://doi.org/10.1175/1520-0426(1998)015<0708:EOTAOP>2.0.CO;2, 1998.

Kovacs, M. and Kirshbaum, D. J.: Topographic impacts on the spatial distribution of deep convection over southern Quebec, J. Appl. Meteorol. Climatol., 55, 743–762, https://doi.org/10.1175/JAMC-D-15-0239.1, 2016.

Kubota, T., Kikuchi, M., Muto, M., Hashimoto, M., Imura, Y., Maruyama, K., Hoffmann, A., Hummel, T., Koopman, R., Malina, E., Rusli, S., Tzallas, V., von Bismarck, J., and Frommknecht, B.: Summary of the EarthCARE science and validation workshop 2025 – Early achievements and future perspectives for the Earth Cloud Aerosol and Radiation Explorer (EarthCARE) satellite mission, J. Eur. Meteorol. Soc., 4, 100037, https://doi.org/10.1016/j.jemets.2026.100037, 2026.

Lachapelle, M., Cholette, M., and Thériault, J. M.: Effect of secondary ice production processes on the simulation of ice pellets using the Predicted Particle Properties microphysics scheme, Atmos. Chem. Phys., 24, 11285–11304, https://doi.org/10.5194/acp-24-11285-2024, 2024.

Li, L., Heymsfield, G. M., Tian, L., and Racette, P. E.: Measurements of Ocean Surface Backscattering Using an Airborne 94 GHz Cloud Radar- Implication for Calibration of Airborne and Spaceborne W-Band Radars, J. Ocean Technol., 22, 1033–1045, https://doi.org/10.1175/JTECH1722.1, 2005.

Liggio, J., Li, S.-M., Staebler, R. M., Hayden, K., Darlington, A., Mittermeier, R. L., O'Brien, J., McLaren, R., Wolde, M., Worthy, D., and Vogel, F.: Measured Canadian oil sands CO_2 emissions are higher than estimates made using internationally recommended methods, Nat. Commun., 10, 1863, https://doi.org/10.1038/s41467-019-09714-9, 2019.

https://doi.org/10.5194/egusphere-2026-5347
Preprint. Discussion started: 9 September 2026

Liu, L., Huang, Y., Qu, Z., Riot-Bretêcher, B., Cole, J., Barker, H., Kacimi, M., Mariani, Z., and Gyakum, J. R.: Validation of EarthCARE cloud microphysical profiles by using ground-based infrared spectral measurements, 2026. (Manuscript in preparation)

McFarquhar, G. M., Ghan, S., Verlinde, J., Korolev, A., Strapp, J. W., Schmid, B., Tomlinson, J. M., Wolde, M., Brooks, S. D., Cziczo, D., Dubey, M. K., Fan, J., Flynn, C., Gultepe, I., Hubbe, J., Gilles, M. K., Laskin, A., Lawson, P., Leaitch, W. R., Liu, P., Liu, X., Lubin, D., Mazzoleni, C., MacDonald, A.-M., Moffet, R. C., Morrison, H., Ovchinnikov, M., Shupe, M. D., Turner, D. D., Xie, S., Zelenyuk, A., Bae, K., Freer, M., and Glen, A.: Indirect and semi-direct aerosol campaign: The impact of Arctic aerosols on clouds, B. Am. Meteorol. Soc., 92, 183–201, https://doi.org/10.1175/2010BAMS2935.1, 2011.

McGill University and Université du Québec à Montréal: Atmospheric and Earth Observation Systems (AEOS) – Climate Sentinel network, available at: https://aeos.meteo.mcgill.ca/, (n.d.) (accessed 2 April 2026).

McTaggart-Cowan, R., Vaillancourt, P. A., Zadra, A., Chamberland, S., Charron, M., Corvec, S., Milbrandt, J. A., Paquin-Ricard, D., Patoine, A., Roch, M., and Separovic, L.: Modernization of atmospheric physics parameterization in Canadian NWP, J. Adv. Model. Earth Syst., 11, 3593–3635, https://doi.org/10.1029/2019MS001781, 2019.

Mariani, Z., Brunet, D., Crawford, R., Reed, R., Holden, S., Sung, K., Michelson, D., Sills, D., Weaver, D., Wang, J., Shrestha, B., Su, Y., Nguyen, C., Bliankinshtein, N., and Wong, K.: The Southern Ontario Lidar (SOLID) Mesonet: Wind and water vapor profiling for aviation and regional nowcasting, J. Atmos. Oceanic Technol., 43, 929–949, https://doi.org/10.1175/JTECH-D-25-0102.1, 2026.

Mariani, Z., Dehghan, A., Joe, P., Sills, D.: Observations of Lake-Breeze Events During the Toronto 2015 Pan-American Games. Boundary-Layer Meteorol 166, 113–135. https://doi.org/10.1007/s10546-017-0289-3, 2018.

Mariani, Z.; Hicks-Jalali, S.; Strawbridge, K.; Gwozdecky, J.; Crawford, R.W.; Casati, B.; Lemay, F.; Lehtinen, R.; Tuominen, P.: Evaluation of Arctic Water Vapor Profile Observations from a Differential Absorption Lidar. Remote Sens. 13, 551. https://doi.org/10.3390/rs13040551, 2021.

Mariani, Z., Huang, L., Crawford, R., Blanchet, J.-P., Hicks-Jalali, S., Mekis, E., Pelletier, L., Rodriguez, P., and Strawbridge, K.: Enhanced automated meteorological observations at the Canadian Arctic Weather Science (CAWS) supersites, Earth Syst. Sci. Data, 14, 4995–5017, https://doi.org/10.5194/essd-14-4995-2022, 2022.

Mariani, Z., Korolev, A., Bliankinshtein, N., Qu, Z., Walker, K. A., Howorucha, M., Cholette, M., Peroni, R., Nguyen, C., Ranjbar, K., Borque, P., and the PONEX Team: Three Canadian aircraft cal/val campaigns in 14 months: ECALOT, WHAFFFERS, and PONEX, EarthCARE Science and Validation Workshop 2026, Oxford, UK, 10 June 2026, presentation, https://airdrive.eventsair.com/eventsairwesteuprod/production-nikal-public/35f40901cb2549e7b7cffea99a9a1639 (last access: 2 September 2026), 2026

https://doi.org/10.5194/egusphere-2026-5347
Preprint. Discussion started: 9 September 2026

Mariani, Z., Morris, S. M., Uttal, T., Akish, E., Crawford, R., Huang, L., Day, J., Tjernström, J., Godøy, Ø., Ferrighi, L., Hartten, L. M., Holt, J., Cox, C. J., O'Connor, E., Pirazzini, R., Maturilli, M., Prakash, G., Mather, J., Strong, K., Fogal, P., Kustov, V., Svensson, G., Gallagher, M., and Vasel, B.: Special Observing Period (SOP) data for the Year of Polar Prediction site Model Intercomparison Project (YOPPsiteMIP), Earth Syst. Sci. Data, 16, 3083–3124, https://doi.org/10.5194/essd-16-3083-2024, 2024.

Mason, S. L., Hogan, R. J., Bozzo, A., and Pounder, N. L.: A unified synergistic retrieval of clouds, aerosols, and precipitation from EarthCARE: the ACM-CAP product, Atmos. Meas. Tech., 16, 3459–3486, https://doi.org/10.5194/amt-16-3459-2023, 2023.

Mayer, J., Gasbarra, D., Hogan, R. J., Malina, E., Mason, S., and Piskala Gvozdikova, B.: EarthCARE reveals details on the role of rain in closed-to-open cell transitions, EGUsphere [preprint], https://doi.org/10.5194/egusphere-2026-3000, 2026.

Milbrandt, J. A., Bélair, S., Faucher, M., Vallée, M., Carrera, M. L., and Glazer, A.: The pan-Canadian high resolution (2.5 km) deterministic prediction system. Wea. Forecasting, 31, 1791–1816, https://doi.org/10.1175/WAF-D-16-0035.1, 2016.

Menekay, D., Kirschler, S., Voigt, C., Wang, Z., Pöhlker, M., Hanstein, I., Kleinbek, T., Sauer, D., De La Torre Castro, E., Jurkat-Witschas, T., and Afchine, A.: Cloud microphysical properties over the Southern Ocean: First results from the HALO-South airborne campaign, EGU General Assembly 2026, Vienna, Austria, 3–8 May 2026, EGU26-13147, https://doi.org/10.5194/egusphere-egu26-13147, 2026.

Minder, J. R., Bassill, N., Fabry, F., French, J. R., Friedrich, K., Gultepe, I., Gyakum, J., Kingsmill, D. E., Kosiba, K., Lachapelle, M., Michelson, D., Nichman, L., Nguyen, C., Thériault, J. M., Winters, A. C., Wolde, M., and Wurman, J.: P-type processes and predictability: The Winter Precipitation Type, Research Multiscale Experiment (WINTRE-MIX), B. Am. Meteorol. Soc., 104, E1469–E1492, https://doi.org/10.1175/BAMS-D-22-0095.1, 2023.

Morrison, H. and Pinto, J. O.: Mesoscale modeling of springtime Arctic mixed-phase stratiform clouds using a new two-moment bulk microphysics scheme, J. Atmos. Sci., 62, 3683–3704, https://doi.org/10.1175/JAS3564.1, 2005.

Mroz, K., Puigdomènech Treserras, B., Battaglia, A., Kollias, P., Tatarevic, A., and Tridon, F.: Cloud and precipitation microphysical retrievals from the EarthCARE Cloud Profiling Radar: the C-CLD product, Atmos. Meas. Tech., 16, 2865–2888, https://doi.org/10.5194/amt-16-2865-2023, 2023.

Mroz, K., Povey, A., Song, R., Pu, Y., Grainger, R., Westbrook, C., Stein, T., and the FAAM Team: Validation of EarthCARE Cloud and Precipitation Products Using FAAM Aircraft Observations: VERIFY campaign, Living Planet Symposium 2025, Vienna, Austria, 23–27 June 2025, presentation, https://lps25.esa.int/lps25-presentations/presentations/844/_844.pdf (last access: 2 September 2026), 2025.

https://doi.org/10.5194/egusphere-2026-5347
Preprint. Discussion started: 9 September 2026

National Academies of Sciences, Engineering, and Medicine (NASEM): Thriving on Our Changing Planet: A Decadal Strategy for Earth Observation from Space, National Academies Press, Washington, DC, https://doi.org/10.17226/24938, 2018.

Nguyen, C. M., Wolde, M., Battaglia, A., Nichman, L., Bliankinshtein, N., Haimov, S., Bala, K., and Schuettemeyer, D.: Coincident in situ and triple-frequency radar airborne observations in the Arctic, Atmos. Meas. Tech., 15, 775–795, https://doi.org/10.5194/amt-15-775-2022, 2022.

O'Neill, N. T., Campanelli, M., Lupu, A., Thulasiraman, S., Reid, J. S., Aube, M., Neary, L., Kaminski, J. W., and McConnell, J. C.: Evaluation of the GEM-AQ air quality model during the Quebec smoke event of 2002: analysis of extensive and intensive optical disparities, Atmos. Environ., 40, 3737–3749, https://doi.org/10.1016/j.atmosenv.2006.03.006, 2006.

Newsom, R. K., Goldsmith, J. E. M., and Sivaraman, C.: Raman Lidar MERGE Value-Added Product, DOE/SC-ARM-TR-189, U.S. Department of Energy, Atmospheric Radiation Measurement (ARM) Program, https://doi.org/10.2172/1353443, 2017.

Protat, A., and Williams, C. R.: The Accuracy of Radar Estimates of Ice Terminal Fall Speed from Vertically Pointing Doppler Radar Measurements. J. Appl. Meteor. Climatol., 50, 2120–2138. https://doi.org/10.1175/JAMC-D-10-05031.1, 2011.

Puigdomènech Treserras, B., Kollias, P. and Battaglia, A.: Retrieval and Climatology of Hydrometeor Sedimentation Velocity from EarthCARE Cloud Profiling Radar Observations, 2026. (Manuscript in preparation)

Qu, Z., Barker, H. W., Cole, J. N. S., and Shephard, M. W.: Across-track extension of retrieved cloud and aerosol properties for the EarthCARE mission: the ACMB-3D product, Atmos. Meas. Tech., 16, 2319–2331, https://doi.org/10.5194/amt-16-2319-2023, 2023.

Qu, Z., Barker, H. W., Korolev, A. V., Milbrandt, J. A., Heckman, I., Bélair, S., Leroyer, S., Vaillancourt, P. A., Wolde, M., Schwarzenböck, A., Leroy, D., Strapp, J. W., Cole, J. N. S., Nguyen, L., and Heidinger, A.: Evaluation of a high-resolution numerical weather prediction model's simulated clouds using observations from CloudSat, GOES-13 and in situ aircraft, Q. J. Roy. Meteor. Soc., 144, 1681–1694, https://doi.org/10.1002/qj.3318, 2018.

Qu, Z., Cholette, M., Korolev, A., Barker, H., Nguyen, C., Borque, P., Ranjbar, K., Peroni, R., Cole, J., Mariani, Z., Kacimi, M., Heckman, I., Milbrandt, J., Bliankinshtein, N., Nichman, L., Bala, K., Blanchet, J.-P., and Blanchard, Y.: Evaluation of NWP simulations of cold-season mixed-phase clouds using EarthCARE and ECALOT observations, EarthCARE 2026 Science and Validation Workshop, Rhodes House, Oxford, UK, 8–12 June 2026, presentation, available at: https://airdrive.eventsair.com/eventsairwesteuprod/production-nikal-public/6eb9d7765a4a4d9bbafff89b68e5874f (last access: 1 September 2026), 2026.

https://doi.org/10.5194/egusphere-2026-5347
Preprint. Discussion started: 9 September 2026

Qu, Z., Korolev, A., Milbrandt, J. A., Heckman, I., Huang, Y., McFarquhar, G. M., Morrison, H., Wolde, M., and Nguyen, C.: The impacts of secondary ice production on microphysics and dynamics in tropical convection, Atmos. Chem. Phys., 22, 12287–12310, https://doi.org/10.5194/acp-22-12287-2022, 2022.

Qu, Z., Korolev, A., Milbrandt, J. A., Heckman, I., Cholette, M., Nguyen, C., and Wolde, M.: The impacts of secondary ice production on the microphysics and dynamics of mid-latitude cold season convection, Atmos. Chem. Phys., 25, 17845–17868, https://doi.org/10.5194/acp-25-17845-2025, 2025.

Qu, Z., Nguyen, C., Barker, H., Borque, P., Korolev, A., Ranjbar, K., Kacimi, M., Cole, J., Heckman, I., Bala, K., Bliankinshtein, N., Nichman, L., Wolde M.: Evaluation of EarthCARE's Scene Construction Algorithm Using Airborne observations, 2026. (Manuscript in preparation)

Roh, W., Satoh, M., Hagihara, Y., Horie, H., Ohno, Y., and Kubota, T.: An evaluation of microphysics in a numerical model using Doppler velocity measured by ground-based radar for application to the EarthCARE satellite, Atmos. Meas. Tech., 17, 3455–3466, https://doi.org/10.5194/amt-17-3455-2024, 2024.

Rugg, A.; Bernstein, B.C.; Haggerty, J.A.; Korolev, A.; Nguyen, C.; Wolde, M.; Heckman, I.; DiVito, S. High Ice Water Content Conditions Associated with Wintertime Elevated Convection in the Midwest. J. Appl. Meteorol. Climatol. 2022, 61, 559–575, https://doi.org/10.1175/JAMC-D-21-0189.1, 2022.

Seiki, T., Horie, H., Hagihara, Y., Aoki, S., and Noda, A. T.: Global identification of dominant ice-particle growth in cirrus clouds using EarthCARE satellite observations, EGUsphere [preprint], https://doi.org/10.5194/egusphere-2025-4819, 2025.

Sioris, C. E., Abboud, I., Fioletov, V. E., and McLinden, C. A.: AEROCAN, the Canadian sub-network of AERONET: Aerosol monitoring and air quality applications, Atmos. Environ., 170, 246–255, https://doi.org/10.1016/j.atmosenv.2017.08.044, 2017.

Stevens, B., Bony, S., Groß, S., Klocke, D., Windmiller, J. M., Wing, A., von Bismarck, J., Brito, E., David, R., Delanoë, J., Farell, D., Wu, Y., et al.: ORCESTRA: Organized Convection and EarthCARE Studies over the Tropical Atlantic, Tellus, 79, 35–52, https://doi.org/10.16993/tellus.4123, 2026.

Stephens, G. L., Vane, D. G., Tanelli, S., Im, E., Durden, S., Rokey, M., Reinke, D., Partain, P., Mace, G. G., Austin, R., Benedetti, A., Mitrescu, C., and the CloudSat Science Team: The CloudSat mission and the A-Train – A new dimension of space-based observations of clouds and precipitation, Bull. Am. Meteorol. Soc., 83, 1771–1790, https://doi.org/10.1175/BAMS-83-12-1771, 2002.

Strapp, J. W., Schwarzenboeck, A., Bedka, K., Bond, T., Calmels, A., Delanoe, J., Dezitter, F., Grzych, M., Harrah, S., Korolev, A., et al.: Comparisons of Cloud In Situ Microphysical Properties of Deep Convective Clouds to Appendix D/P Using

https://doi.org/10.5194/egusphere-2026-5347
Preprint. Discussion started: 9 September 2026

Data from the High-Altitude Ice Crystals-High Ice Water Content and High Ice Water Content-RADAR I Flight Campaigns, SAE Int. J. Aerospace, 14, 127–159, https://doi.org/10.4271/01-14-02-0007, 2021.

van Gelder, L., Kollias, P., Mech, M., Pfitzenmaier, L., and Crewell, S.: Validating EarthCARE's CPR in the Arctic: Results from the COMPEX-EC Airborne Campaign, EarthCARE Science and Validation Workshop 2025, Tokyo, Japan, 1–5 December 2025, presentation, https://www.eorc.jaxa.jp/EARTHCARE/event/ws2025/program-data/H426_vanGelder.pdf (last access: 2 September 2026), 2025.

Várnai, T. and Marshak, A.: A method for analyzing how various parts of clouds influence each other's brightness, J. Geophys. Res. Atmos., 108, 4706, https://doi.org/10.1029/2003JD003561, 2003.Velázquez Blázquez, A., Domenech, C., Baudrez, E., Clerbaux, N., Salas Molar, C., and Madenach, N.: Retrieval of top-of-atmosphere fluxes from combined EarthCARE lidar, imager, and broadband radiometer observations: the BMA-FLX product, Atmos. Meas. Tech., 17, 7007–7026, https://doi.org/10.5194/amt-17-7007-2024, 2024.

Villefranque, N., Blanco, S., Couvreux, F., Fournier,Gautrais, J., Hogan, R. J., et al.: Process-based climate model development harnessing machine learning: III. The representation of cumulus geometry and their 3-D radiative effects, J. Adv. Model. Earth Syst., 13, e2020MS002423, https://doi.org/10.1029/2020MS002423, 2021.

Walker, K. A., Mariani, Z., Korolev, A., Qu, Z., Bliankinshtein, N., Nguyen, C., Nichman, L., Wolde, M., Strong, K., Bourassa, A., Blanchet, J.-P., and the PONEX Team: An overview of the Polar Night Experiment (PONEX) aircraft campaign for HAWC and EarthCARE, EarthCARE Science and Validation Workshop 2025, Tokyo, Japan, 1–5 December 2025, presentation, https://www.eorc.jaxa.jp/EARTHCARE/event/ws2025/program-data/H425_Walker.pdf (last access: 2 September 2026), 2025.

Wandinger, U., Haarig, M., Baars, H., Donovan, D., and van Zadelhoff, G.-J.: Cloud top heights and aerosol layer properties from EarthCARE lidar observations: the A-CTH and A-ALD products, Atmos. Meas. Tech., 16, 4031–4052, https://doi.org/10.5194/amt-16-4031-2023, 2023.

Wehr, T.: EarthCARE Product Validation Requirements Document Level 1b/c and Level 2a/b Products, available at: https://earth.esa.int/eogateway/documents/20142/37627/EarthCARE-Validation-Requirements.pdf. (accessed 17 February 2026), 2017.

Wehr, T., Kubota, T., Tzeremes, G., Wallace, K., Nakatsuka, H., Ohno, Y., Koopman, R., Rusli, S., Kikuchi, M., Eisinger, M., Tanaka, T., Taga, M., Deghaye, P., Tomita, E., and Bernaerts, D.: The EarthCARE mission – science and system overview, Atmos. Meas. Tech., 16, 3581–3608, https://doi.org/10.5194/amt-16-3581-2023, 2023.

Winker, D. M., Pelon, J., Coakley Jr., J. A., Ackerman, S. A., Charlson, R. J., Colarco, P. R., Flamant, P., Fu, Q., Hoff, R. M., Kittaka, C., Kubar, T. L., Le Treut, H., McCormick, M. P., Mégie, G., Poole, L. R., Powell, K., Trepte, C. R., Vaughan, M.

A., and Wielicki, B. A.: The CALIPSO mission: A global 3D view of aerosols and clouds, Bull. Am. Meteorol. Soc., 91, 1211–1229, https://doi.org/10.1175/2010BAMS3009.1, 2010.

Wolde, M., Battaglia, A., Nguyen, C., Pazmany, A. L., and Illingworth, A.: Implementation of polarization diversity pulse-pair technique using airborne W-band radar, Atmos. Meas. Tech., 12, 253–269, https://doi.org/10.5194/amt-12-253-2019, 2019.

Xu, Z., Kollias, P., Sasikumar, S., Battaglia, A., and Puigdomènech Treserras, B.: EarthCARE Cloud Profiling Radar Observations of the Vertical Structure of Marine Stratocumulus Clouds, EGUsphere [preprint], https://doi.org/10.5194/egusphere-2025-5421, 2025.